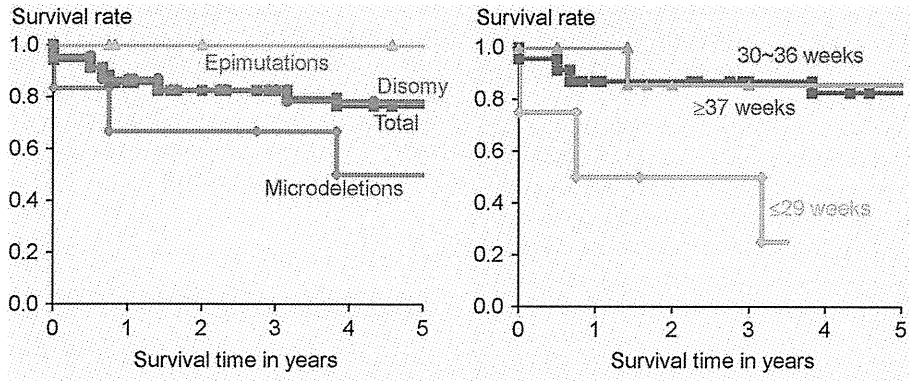

Patient	(Epi)genetic cause	GA	Cause of death	Age of death
1	UPD(14)pat (S-1)	34	Respiratory failure	2 hours
8	UPD(14)pat (S-1)	24	Influenza infection	3 2/12 yrs
15	UPD(14)pat (S-3)	34	Necrotizing enterocolitis	6 mos
17	UPD(14)pat (S-3)	32	Hepatoblastoma	8 mos
18	UPD(14)pat (S-3)	37	Hemophagocytic syndrome	1 5/12 yrs
30	Microdeletion (S-1)	27	Sudden death at URI	9 mos
32	Microdeletion (S-2)	28	Intracranial hemorrhage	4 days
33	Microdeletion (S-3)	35	RS virus infection	3 10/12 yrs

Figure 5 Kaplan–Meier survival curves according to the (epi)genetic cause and the gestational age (week), and summary of the causes of death. GA, gestational age; URI, upper respiratory infection; and RS, respiratory syncytial. Patients #8, #17, and #18 had hepatoblastoma.

The present study revealed several notable findings. First, polyhydramnios was identified during the pregnancies of nearly all patients, except for patient #32 of Del-S2. Amniotic fluid originates primarily from fetal urine and is absorpted primarily by fetal swallowing into the digestive system.[18,19] Since fetal hydration and the resultant urine flow mainly depend on the water flow from maternal circulation across the placenta,[19] placentomegaly would have facilitated the production of amniotic fluid. Furthermore, since feeding difficulty with impaired swallowing was observed in most patients, defective swallowing would have compromised absorption of amniotic fluid. Thus, both body and placental factors are assumed for the development of polyhydramnios. This would explain why polyhydramnios was observed in patients #1, #6, and #8 who were free from placentomegaly, and in patient #22 who showed no feeding difficulty, although the presence of feeding difficulty was unknown for patient #1 as was placentomegaly for patient #22. In addition, since amniotic fluid begins to increase from 8–11 weeks of gestation and reaches its maximum volume around 32 weeks of gestation,[18,19] this would explain why amnioreduction was usually required from 30 weeks of gestation.

Second, birth size was relatively well preserved, whereas postnatal growth was rather compromised. The well preserved prenatal growth in apparently compromised intrauterine environments would be consistent with the conflict theory that overexpression of *PEGs* promotes fetal and placental growth.[20] Notably, birth weight was disproportionately greater than birth length in the apparent absence of generalized edema. In this regard, mouse *Dlk1*, *Rtl1*, and *Gtl2* (*Meg3*) on the distal part of chromosome 12 are expressed in skeletal muscles (Supplementary Figure S5),[14,17] and paternal disomy for chromosome 12 causes muscular hypertrophy.[21] Thus, patients with UPD(14)pat and related conditions may have muscular hypertrophy especially in the fetal life. The compromised postnatal growth would primarily be because of poor nutrition caused by feeding difficulties, whereas relative overweight suggestive of possible muscular hypertrophy remains to be recognized.

Third, DD/ID was invariably present in all 26 patients examined for their developmental/intellectual status, with the median DQ/IQ of 55. In this regard, mouse *Dlk1*, *Rtl1*, and *Gtl2* (*Meg3*) are expressed in the brain during embryogenesis (Supplementary Figure S5),[22] and *Dlk1* is involved in the differentiation of midbrain dopaminergic neurons.[22] Thus, DD/ID would primarily be ascribed to the altered expression dosage of *PEGs/MEGs* in the brain.

Fourth, hepatoblastoma was identified in three patients of UPD-group during infancy. In this context, it has been reported that (1) mouse *Dlk1*, *Rtl1*, and *Meg3* (*Gtl2*) are expressed in the fetal liver, but not in the adult liver; [14,17,23,24] (2) overexpression of *Rtl1* in the adult mouse liver has induced hepatic tumors with high penetrance;[24] (3) *Meg3* functions as a tumor suppressor gene in mice;[25] (4) human *DLK1* is expressed in the hepatocytes of 5–6 weeks old embryos;[26] and (5) human DLK1 protein is upregulated in hepatoblastoma.[27] These findings imply the relevance of excessive *RTL1* expression and loss of *MEG3* expression to the occurrence of hepatoblastoma in UPD(14)pat and related conditions, while it remains to be determined whether the DLK1 upregulation is the cause or the result of hepatoblastoma development. Thus, periodical screening for hepatoblastoma, such as serum α-fetoprotein measurement and abdominal ultrasonography, is recommended. In this context, it remains to be studied whether other embryonal tumors may also be prone to occur in UPD(14)pat and related conditions.

Fifth, mortality was high in Del-group and null in Epi-group. The high mortality in Del-group would primarily be ascribed to the high prevalence of premature delivery, although it is unknown whether the high prevalence of premature delivery is an incidental finding or characteristic of Del-group. The null mortality in Epi-group may be due to possible mosaicism with cells accompanied by a normal expression pattern because of escape from epimutation, as reported previously.[28,29] It is unknown, however, whether possible presence of trisomic cells in TR-mediated UPD(14)pat and that of normal cells in PE-mediated UPD(14) may have exerted clinical effects. Notably, since

death was observed only in patients <4 years of age, the vital prognosis is expected to be good from childhood. In addition, since three patients died during respiratory infections, careful management is recommended during such infections.

Furthermore, the present study also provides several useful clinical implications: (1) two patients had Robertsonian translocations as a risk factor for the development of UPD.[30] Thus, karyotyping is suggested for patients with an UPD(14)pat-like phenotype; (2) prenatal detection of polyhydramnios and thoracic and abdominal features is possible from ~25 weeks of gestation; (3) mechanical ventilation and gastric tube feeding are usually required, with variable durations; (4) there was no patient in UPD-group who exhibited clinical features that are attributable to the unmasking of a recessive mutation(s) of paternal origin; (5) since UPD(14)pat and related conditions share several clinical features including embryonal tumors with BWS (Supplementary Table S4), UPD(14)pat and related conditions may be worth considering in atypical or underlying factor-unknown BWS; and (6) since clinical findings are comparable between patients examined in this study and 17 similarly affected non-Japanese patients (Supplementary Table S5), our data will be applicable to non-Japanese patients as well.

A critical matter for UPD(14)pat and related conditions is the lack of a syndrome name. Although the term 'UPD(14)pat syndrome' has been utilized previously,[4] the term is confusing because 'UPD(14)pat syndrome' can be caused by (epi)genetic mechanisms other than UPD (14)pat. In this regard, the name 'Temple syndrome' has been proposed for UPD(14)mat and related conditions or 'UPD(14)mat syndrome',[31,32] a mirror image of UPD(14)pat and related conditions. On the basis of our previous and present studies that have made a significant contribution to the clarification of underlying (epi)genetic factors and the definition of clinical findings, we would propose the name 'Kagami–Ogata syndrome', or 'Wang–Kagami–Ogata syndrome' with the name of Wang who first described UPD(14)pat,[33] for UPD (14)pat and related conditions.

In summary, although the number of patients still remains small, especially in each subtype of Del-group, the present study reveals pathognomic and characteristic clinical findings in UPD(14)pat and related conditions. Furthermore, this study shows the invariable occurrence of DD/ID and the occasional (8.8%) development of hepatoblastoma, thereby showing the necessity of adequate support for DD/ID and screening of hepatoblastoma in affected patients. Finally, we propose the name 'Kagami–Ogata syndrome' for UPD(14)pat and related conditions.

CONFLICT OF INTEREST

The authors declare no conflict of interest.

ACKNOWLEDGEMENTS

We are grateful to all patients and their parents for their cooperation. We thank Drs Haruhiko Sago, Aiko Sasaki, Jun Shibasaki, Rika Kosaki, Michiko Hayashidani, Toshio Takeuchi, Shinya Tanaka, Mika Noguchi, Goro Sasaki, Kouji Masumoto, Takeshi Utsunomiya, Yumiko Komatsu, Hirofumi Ohashi, Hiroshi Kishimoto, Maureen J O'Sullivan, Andrew J Green, Yoshiyuki Watabe, Tsuyako Iwai, Hitoshi Kawato, Akiko Yamamoto, Nobuhiro Suzumori, Hiroko Ueda, Makoto Kuwajima, Kiyoko Samejima, Hiroshi Yoshihashi, Yoriko Watanabe, Jin Nishimura, Shuku Ishikawa, Michiko Yamanaka, Machiko Nakagawa, Hiroharu Inoue, Takashi Imamura, Keiichi Motoyama and Ryoko Yoshinare for providing us with detailed clinical data and materials for molecular studies, Dr Gen Nishimura for interpretation of roentgengraphic findings, and Drs Tadayuki Ayabe, Keiko Matsubara, Yoichi Sekita and Maki Fukami for their support in molecular analyses. We also thank Ms. Emma Barber for her editorial assistance with the final draft of this paper. This work was supported by Grants-in-Aid for Scientific Research (A) (25253023) and Research (B) (23390083) from the Japan Society for the Promotion of Science (JSPS), and by Grants for Health Research on Children, Youth, and Families (H25-001) and for Research on Intractable Diseases (H22-161) from the Ministry of Health, Labor and Welfare (MHLW), by Grants from the National Center for Child Health and Development (23A-1, 25-10), and by Grant from Takeda Science Foundation.

1 da Rocha ST, Edwards CA, Ito M, Ogata T, Ferguson-Smith AC: Genomic imprinting at the mammalian Dlk1-Dio3 domain. *Trends Genet* 2008; **24**: 306–316.
2 Kagami M, Sekita Y, Nishimura G *et al*: Deletions and epimutations affecting the human 14q32.2 imprinted region in individuals with paternal and maternal upd(14)-like phenotypes. *Nat Genet* 2008; **40**: 237–242.
3 Kagami M, O'Sullivan MJ, Green AJ *et al*: The IG-DMR and the MEG3-DMR at human chromosome 14q32.2: hierarchical interaction and distinct functional properties as imprinting control centers. *PLoS Genet* 2010; **6**: e1000992.
4 Beygo J, Elbracht M, de Groot K *et al*: Novel deletions affecting the MEG3-DMR provide further evidence for a hierarchical regulation of imprinting in 14q32. *Eur J Hum Genet* 2015; **23**: 180–188.
5 Hoffmann K, Heller R: Uniparental disomies 7 and 14. *Best Pract Res Clin Endocrinol Metab* 2011; **25**: 77–100.
6 Kagami M, Matsuoka K, Nagai T *et al*: Paternal uniparental disomy 14 and related disorders: placental gene expression analyses and histological examinations. *Epigenetics* 2012; **7**: 1142–1150.
7 Kurosawa K, Sasaki H, Sato Y *et al*: Paternal UPD14 is responsible for a distinctive malformation complex. *Am J Med Genet* 2002; **110**: 268–272.
8 Kagami M, Nishimura G, Okuyama T *et al*: Segmental and full paternal isodisomy for chromosome 14 in three patients: narrowing the critical region and implication for the clinical features. *Am J Med Genet A* 2005; **138A**: 127–132.
9 Kagami M, Kato F, Matsubara K, Sato T, Nishimura G, Ogata T: Relative frequency of underlying genetic causes for the development of UPD(14)pat-like phenotype. *Eur J Hum Genet* 2012; **20**: 928–932.
10 Horii M, Horiuchi H, Momoeda M, Nakagawa M *et al*: Hepatoblastoma in an infant with paternal uniparental disomy 14. *Congenit Anom (Kyoto)* 2012; **52**: 219–220.
11 Miyazaki O, Nishimura G, Kagami M, Ogata T: Radiological evaluation of dysmorphic thorax of paternal uniparental disomy 14. *Pediatr Radiol* 2011; **41**: 1013–1019.
12 Parveen Z, Tongson-Ignacio JE, Fraser CR, Killeen JL, Thompson KS: Placental mesenchymal dysplasia. *Arch Pathol Lab Med* 2007; **131**: 131–137.
13 Williams DH, Gauthier DW, Maizels M: Prenatal diagnosis of Beckwith–Wiedemann syndrome. *Prenat Diagn* 2005; **25**: 879–884.
14 da Rocha ST, Tevendale M, Knowles E, Takada S, Watkins M, Ferguson-Smith AC: Restricted co-expression of Dlk1 and the reciprocally imprinted non-coding RNA, Gtl2: implications for cis-acting control. *Dev Biol* 2007; **306**: 810–823.
15 da Rocha ST, Charalambous M, Lin SP *et al*: Gene dosage effects of the imprinted delta-like homologue 1 (dlk1/pref1) in development: implications for the evolution of imprinting. *PLoS Genet* 2009; **5**: e1000392.
16 Sekita Y, Wagatsuma H, Nakamura K *et al*: Role of retrotransposon-derived imprinted gene, Rtl1, in the feto-maternal interface of mouse placenta. *Nat Genet* 2008; **40**: 243–248.
17 Brandt J, Schrauth S, Veith AM *et al*: Transposable elements as a source of genetic innovation: expression and evolution of a family of retrotransposon-derived neogenes in mammals. *Gene* 2005; **345**: 101–111.
18 Modena AB, Fieni S: Amniotic fluid dynamics. *Acta Biomed* 2004; **75**: 11–13.
19 Beall MH, van den Wijngaard JP, van Gemert MJ, Ross MG: Amniotic fluid water dynamics. *Placenta* 2007; **28**: 816–823.
20 Hurst LD, McVean GT: Growth effects of uniparental disomies and the conflict theory of genomic imprinting. *Trends Genet* 1997; **13**: 436–443.
21 Georgiades P, Watkins M, Surani MA, Ferguson-Smith AC: Parental origin-specific developmental defects in mice with uniparental disomy for chromosome 12. *Development* 2000; **127**: 4719–4728.
22 Wilkinson LS, Davies W, Isles AR: Genomic imprinting effects on brain development and function. *Nat Rev Neurosci* 2007; **8**: 832–843.
23 Kang ER, Iqbal K, Tran DA *et al*: Effects of endocrine disruptors on imprinted gene expression in the mouse embryo. *Epigenetics* 2011; **6**: 937–950.
24 Riordan JD, Keng VW, Tschida BR *et al*: Identification of rtl1, a retrotransposon-derived imprinted gene, as a novel driver of hepatocarcinogenesis. *PLoS Genet* 2013; **9**: e1003441.
25 Zhou Y, Zhang X, Klibanski A: MEG3 noncoding RNA: a tumor suppressor. *J Mol Endocrinol* 2012; **48**: R45–R53.
26 Floridon C, Jensen CH, Thorsen P *et al*: Does fetal antigen 1 (FA1) identify cells with regenerative, endocrine and neuroendocrine potentials? A study of FA1 in embryonic, fetal, and placental tissue and in maternal circulation. *Differentiation* 2000; **66**: 49–59.
27 Falix FA, Aronson DC, Lamers WH, Hiralall JK, Seppen J: DLK1, a serum marker for hepatoblastoma in young infants. *Pediatr Blood Cancer* 2012; **59**: 743–745.
28 Yamazawa K, Kagami M, Fukami M, Matsubara K, Ogata T: Monozygotic female twins discordant for Silver-Russell syndrome and hypomethylation of the H19-DMR. *J Hum Genet* 2008; **53**: 950–955.

29 Azzi S, Blaise A, Steunou V *et al*: Complex tissue-specific epigenotypes in Russell–Silver Syndrome associated with 11p15 ICR1 hypomethylation. *Hum Mutat* 2014; **35**: 1211–1220.
30 Berend SA, Horwitz J, McCaskill C, Shaffer LG: Identification of uniparental disomy following prenatal detection of Robertsonian translocations and isochromosomes. *Am J Hum Genet* 2000; **66**: 1787–1793.
31 Ioannides Y, Lokulo-Sodipe K, Mackay DJ, Davies JH, Temple IK: Temple syndrome: improving the recognition of an underdiagnosed chromosome 14 imprinting disorder: an analysis of 51 published cases. *J Med Genet* 2014; **51**: 495–501.
32 Hosoki K, Kagami M, Tanaka T *et al*: Maternal uniparental disomy 14 syndrome demonstrates Prader–Willi syndrome-like phenotype. *J Pediatr* 2009; **155**: 900–903.
33 Wang JC, Passage MB, Yen PH, Shapiro LJ, Mohandas TK: Uniparental heterodisomy for chromosome 14 in a phenotypically abnormal familial balanced 13/14 Robertsonian translocation carrier. *Am J Hum Genet* 1991; **48**: 1069–1074.
34 Kagami M, Yamazawa K, Matsubara K *et al*: Placentomegaly in paternal uniparental disomy for human chromosome 14. *Placenta* 2008; **29**: 760–761.

Supplementary Information accompanies this paper on European Journal of Human Genetics website (http://www.nature.com/ejhg)

ORPHANET JOURNAL OF RARE DISEASES

RESEARCH Open Access

Japanese founder duplications/triplications involving *BHLHA9* are associated with split-hand/foot malformation with or without long bone deficiency and Gollop-Wolfgang complex

Eiko Nagata[1†], Hiroki Kano[2†], Fumiko Kato[1], Rie Yamaguchi[1], Shinichi Nakashima[1], Shinichiro Takayama[3], Rika Kosaki[4], Hidefumi Tonoki[5], Seiji Mizuno[6], Satoshi Watanabe[7], Koh-ichiro Yoshiura[7], Tomoki Kosho[8], Tomonobu Hasegawa[9], Mamori Kimizuka[10], Atsushi Suzuki[11], Kenji Shimizu[11], Hirofumi Ohashi[11], Nobuhiko Haga[12], Hironao Numabe[13], Emiko Horii[14], Toshiro Nagai[15], Hiroshi Yoshihashi[16], Gen Nishimura[17], Tatsushi Toda[18], Shuji Takada[19], Shigetoshi Yokoyama[19,22], Hiroshi Asahara[19,20], Shinichiro Sano[1,21], Maki Fukami[21], Shiro Ikegawa[2] and Tsutomu Ogata[1*]

Abstract

Background: Limb malformations are rare disorders with high genetic heterogeneity. Although multiple genes/loci have been identified in limb malformations, underlying genetic factors still remain to be determined in most patients.

Methods: This study consisted of 51 Japanese families with split-hand/foot malformation (SHFM), SHFM with long bone deficiency (SHFLD) usually affecting the tibia, or Gollop-Wolfgang complex (GWC) characterized by SHFM and femoral bifurcation. Genetic studies included genomewide array comparative genomic hybridization and exome sequencing, together with standard molecular analyses.

Results: We identified duplications/triplications of a 210,050 bp segment containing *BHLHA9* in 29 SHFM patients, 11 SHFLD patients, two GWC patients, and 22 clinically normal relatives from 27 of the 51 families examined, as well as in 2 of 1,000 Japanese controls. Families with SHFLD- and/or GWC-positive patients were more frequent in triplications than in duplications. The fusion point was identical in all the duplications/triplications and was associated with a 4 bp microhomology. There was no sequence homology around the two breakpoints, whereas rearrangement-associated motifs were abundant around one breakpoint. The rs3951819-*D17S1174* haplotype patterns were variable on the duplicated/triplicated segments. No discernible genetic alteration specific to patients was detected within or around *BHLHA9*, in the known causative SHFM genes, or in the exome.

(Continued on next page)

* Correspondence: tomogata@hama-med.ac.jp
†Equal contributors
[1]Department of Pediatrics, Hamamatsu University School of Medicine, Hamamatsu 431-3192, Japan
Full list of author information is available at the end of the article

(Continued from previous page)

Conclusions: These results indicate that *BHLHA9* overdosage constitutes the most frequent susceptibility factor, with a dosage effect, for a range of limb malformations at least in Japan. Notably, this is the first study revealing the underlying genetic factor for the development of GWC, and demonstrating the presence of triplications involving *BHLHA9*. It is inferred that a Japanese founder duplication was generated through a replication-based mechanism and underwent subsequent triplication and haplotype modification through recombination-based mechanisms, and that the duplications/triplications with various haplotypes were widely spread in Japan primarily via clinically normal carriers and identified via manifesting patients. Furthermore, genotype-phenotype analyses of patients reported in this study and the previous studies imply that clinical variability is ascribed to multiple factors including the size of duplications/triplications as a critical factor.

Keywords: *BHLHA9*, Split-hand/foot malformation, Long bone deficiency, Gollop-Wolfgang complex, Expressivity, Penetrance, Susceptibility, Japanese founder copy number gain

Introduction

Split-hand/foot malformation (SHFM), also known as ectrodactyly, is a rare limb malformation involving the central rays of the autopod [1,2]. It presents with median clefts of the hands and feet, aplasia/hypoplasia of the phalanges, metacarpals, and metatarsals, and syndactyly. SHFM results from failure to maintain the central portion of the apical ectodermal ridge (AER) in the developing autopod [1,2]. SHFM is divided into two forms: a non-syndromic form with limb-confined manifestations and a syndromic form with extra-limb manifestations [2]. Furthermore, non-syndromic SHFM can occur as an isolated abnormality confined to digits (hereafter, SHFM refers to this type) or in association with other limb abnormalities as observed in SHFM with long bone deficiency (SHFLD) usually affecting the tibia and in Gollop-Wolfgang complex (GWC) characterized by femoral bifurcation [1,2]. Both syndromic and non-syndromic forms are associated with wide expressivity and penetrance even among members of a single family and among limbs of a single patient [2].

SHFM and SHFLD are genetically heterogeneous conditions reviewed in ref. [2]. To date, SHFM has been identified in patients with heterozygous deletions or translocations involving the *DLX5–DLX6* locus at 7q21.2–21.3 (SHFM1) [3] (*DLX5* mutations have been detected recently), heterozygous duplications at 10q24 (SHFM3), heterozygous mutations of *TP63* at 3q27 (SHFM4), heterozygous deletions affecting *HOXD* cluster at 2q31 (SHFM5), and biallelic mutations of *WNT10B* at 12q31 (SHFM6); in addition, SHFM2 has been assigned to Xq26 by linkage analyses in a large Pakistani kindred [2]. Similarly, a genomewide linkage analysis in a large consanguineous family has identified two SHFLD susceptibility loci, one at 1q42.2–q43 (SHFLD1) and the other at 6q14.1 (SHFLD2); furthermore, after assignment of another SHFLD locus to 17p13.1–13.3 [4], duplications at 17p13.3 (SHFLD3) have been found in patients with SHFLD reviewed in ref. [2]. However, the GWC locus (loci) remains unknown at present.

The duplications at 17p13.3 identified to date are highly variable in size, and harbor *BHLHA9* as the sole gene within the smallest region of overlap [5-9]. *Bhlha9*/*bhlha9* is expressed in the limb bud mesenchyme underlying the AER in mouse and zebrafish embryos, and *bhlha9* knockdown has resulted in shortening of the pectoral fins in zebrafish [6]. Furthermore, *BHLHA9*-containing duplications have been identified not only in patients with SHFLD but also in those with SHFM and clinically normal family members [4-10]. These findings argue for a critical role of *BHLHA9* duplication in the development of SHFM and SHFLD, with variable expressivity and incomplete penetrance.

In this study, we report on *BHLHA9*-containing duplications/triplications with an identical fusion point and various haplotype patterns that were associated with a range of limb malformations including GWC, and discuss on characteristic clinical findings, genomic basis of Japanese founder copy number gains, and underlying factors for phenotypic variability.

Materials and methods

Patients/subjects

We studied 68 patients with SHFM (n = 55), SHFLD (n = 11), or GWC (n = 2), as well as 60 clinically normal relatives, from 51 Japanese families; the pedigrees of 27 of the 51 families and representative clinical findings are shown in Figure 1. All the probands 1–51 had a normal karyotype. Southern blot analysis for SHFM3 locus had been performed in 28 probands with SHFM, indicating 10q24 duplications in two of them [11]. Clinical features including photographs and roentgenograms of a proband with GWC and his brother with SHFLD (family 23 in Figure 1A) were as described previously [12]. The residencies of families 1–51 were widely distributed throughout Japan.

Ethical approval and samples

This study was approved by the Institutional Review Board Committees of Hamamatsu University School of

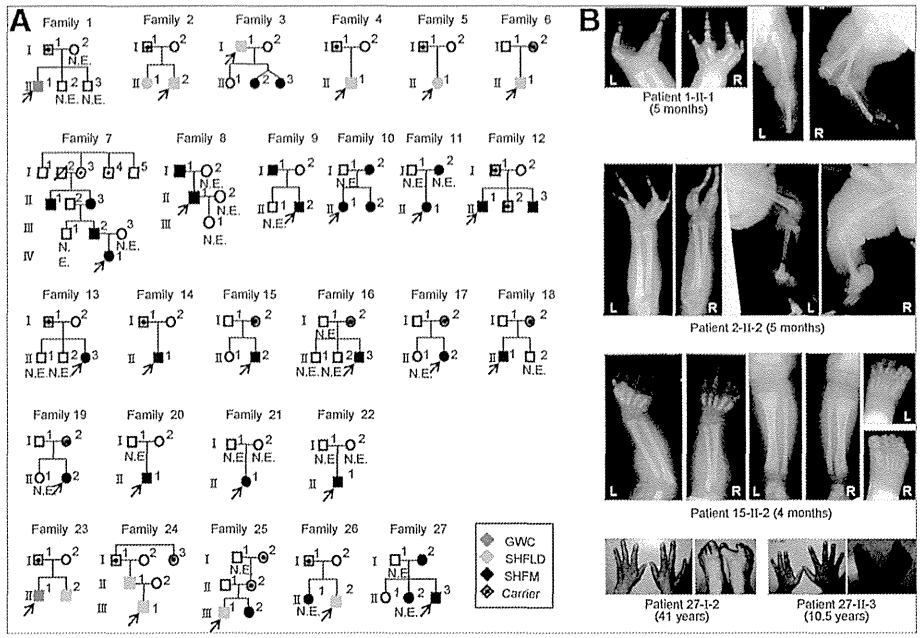

Figure 1 Clinical summary. A. Pedigrees of 27 Japanese families with duplications (families 1–22) and triplications (families 23–27) of a ~200 kb region involving *BHLHA9*. The duplications/triplications are associated with GWC, SHFLD, SHFM, or normal phenotype (carriers). N.E.: Not examined molecularly. **B**. Representative clinical findings. Each patient is indicated by a family-generation-individual style and corresponds to the patient/subject shown in Figure 1A and Additional file 5. The top panel: GWC with right bifid femur; the second panel: SHFLD with bilateral tibial deficiencies, the third panel: SHFM with polydactyly; and the bottom panel: SHFM.

Medicine, RIKEN, and National Center for Child Health and Development, and was performed using peripheral leukocyte samples after obtaining written informed consent for the molecular analysis and the publication of genetic and clinical data after removing information for personal identification (e.g., name, birthday, and facial photograph) from the adult subjects (^{3} 20 years) or from the parents of the child subjects (below 20 years). Furthermore, informed assent was also obtained from child subjects between 6–20 years.

Samples and primers

The primers utilized in this study are summarized in Additional file 1.

Molecular studies

Sanger sequencing, fluorescence *in situ* hybridization (FISH), microsatellite genotyping, Southern blotting, and bisulfite sequencing-based methylation analysis were performed by the standard methods, as reported previously [13]. Quantitative real-time PCR (qPCR) analysis was carried out by the SYBR Green methods on StepOnePlus system, using *RNaseP* as an internal control (Life Technologies). Genomewide oligonucleotide-based array comparative genomic hybridization (CGH) was performed with a catalog human array (4 × 180 K format, ID G4449A) according to the manufacturer's instructions (Agilent Technologies), and obtained copy number variants/polymorphisms were screened with Agilent Genomic Workbench software using the Database of Genomic Variants (http://dgv.tcag.ca/dgv/app/home). Sequencing of a long region encompassing *BHLHA9* was performed with the Nextera XT kit on MiSeq (Illumina), using SAMtools v0.1.17 software (http://samtools.sourceforge.net/). Exome sequencing was performed as described previously [14].

Assessment of genomic environments around the fusion points

Repeat elements around the fusion point were searched for using Repeatmasker (http://www.repeatmasker.org). Rearrangement-inducing DNA features were investigated for 300 bp regions at both the proximal and the distal sides of each breakpoint, using GEECEE (http://emboss.bioinformatics.nl/cgi-bin/emboss/geecee) for calculation of the average GC content, PALINDROME (http://mobyle.pasteur.fr/cgi-bin/portal.py#forms::palindrome) and Non-B DB (http://nonb.abcc.ncifcrf.gov) for the examination of the palindromes and non-B (non-canonical) structures, and Fuzznuc (http://emboss.bioinformatics.nl/cgi-bin/emboss/fuzznuc) for the assessment of rearrangement-associated sequence motifs and tri/tetranucleotides [15-20]. For controls, we examined 48 regions of 600 bp long selected at an interval of 1.5 Mb from the entire chromosome 17.

Statistical analysis

The statistical significance of the frequency was analyzed by the two-sided Fisher's exact probability test.

Results

Sequence analysis of the known causative/candidate genes

We performed direct sequencing for the previously known causative genes (*DLX5*, *TP63*, and *WNT10B*) reviewed in ref. [2] in the probands 1–51. Although no pathologic mutation was identified in *DLX5* and *TP63*, the previously reported homozygous missense mutation of *WNT10B* (c.944C > T, p.R332W) [21] was detected in the proband 48 with SHFM who was born to healthy consanguineous parents heterozygous for this mutation. In addition, while no variation was detected in *DLX5* and *WNT10B*, rs34201045 (4 bp insertion polymorphism) in *TP63* [21] was detected with an allele frequency of 61%.

We also examined *BHLHA9*, because gain-of-function mutations of *BHLHA9* as well as *BHLHA9*-harboring duplications may lead to limb malformations. No sequence variation was identified in the 51 probands.

Array CGH analysis

Array CGH analysis was performed for the probands 1–51, showing increased copy numbers at 17p13.3 encompassing *BHLHA9* (SHFLD3) in the probands 1–27 from families 1–27 (Figure 1A). Furthermore, heterozygous duplications at 10q24 (SHFM3) were detected in the probands 49–51, i.e., a hitherto unreported patient with paternally inherited SHFM (his father also had the duplication) and the two patients who had been indicated to have the duplications by Southern blot analysis [11]. No copy number alteration was observed at other SHFM/SHFLD loci in the probands 1–27 and 49–51. In the remaining probands 28–48, there was no copy number variation that was not registered in the Database of Genomic Variants.

Identical fusion points in *BHLHA9*-containing duplications/triplications

The array CGH indicated that the increased copy number regions at 17p13.3 were quite similar in the physical size in the probands 1–27 and present in three copies in the probands 1–22 and in four copies in the probands 23–27 (Figure 2A). Thus, FISH analysis was performed using 8,259 bp PCR products amplified from this region, showing two signals with a different intensity that was more obvious in the probands 23–27 (Figure 2A).

We next determined the fusion points of the duplications/triplications (Figure 2B). PCR products of 2,195 bp long were obtained with P1/P2 primers in the probands 1–27, and the fusion point was determined by direct sequencing for 418 bp PCR products obtained with P3/P4 primers. The fusion point was identical in all the probands 1–27; it resided on intron 1 of *ABR* and intron 1 of *YWHAE*, and was associated with a 4 bp microhomology.

Then, we performed qPCR analysis for a 214 bp region harboring the fusion point, using P5/P6 primers (Figure 2C and Additional file 2). The fusion point was present in a single copy in the probands 1–22 and in two copies in the probands 23–27. The results showed that the identical genomic segment harboring *BHLHA9* was tandemly duplicated in the probands 1–22 and triplicated in the probands 23–27. According to GRCh37/hg19 (http://genome.ucsc.edu/), the genomic segment was 210,050 bp long.

We also performed array CGH and qPCR for the fusion point in 15 patients other than the probands and 47 clinically normal relatives from the 27 families (Figures 1 and 2C). The duplications/triplications were identified in all the 15 patients. Thus, in a total of 42 patients, duplications/triplications were found in 29 SHFM patients, 11 SHFLD patients, and two GWC patients. Furthermore, the duplications/triplications were also present in 22 of the 47 clinically normal relatives. In particular, they were invariably identified in either of the clinically normal parents when both of them were examined; they were also present in other clinically normal relatives in families 7, 12, 24, and 25.

Since the above data indicated the presence of duplications/triplications in clinically normal subjects, we performed qPCR for the fusion point in 1,000 Japanese controls. The fusion point was detected in a single copy in two subjects (Subjects 1 and 2 in Figure 2C). We also performed array CGH in 200 of the 1,000 controls including the two subjects, confirming the duplications in the two subjects and lack of other copy number variations, including deletions involving *BHLHA9*, which were not registered in the Database of Genomic Variants in the 200 control subjects. The frequency of duplications/triplications was significantly higher in the probands than in the control subjects (27/51 vs. 2/1,000, $P = 3.5 \times 10^{-37}$).

Various haplotype patterns on the duplicated/triplicated segments

We carried out genotyping for rs3951819 (A/G SNP on *BHLHA9*) and *D17S1174* (CA repeat microsatellite locus) on the genomic segment subjected to duplications/triplications (Figure 2A), and determined rs3951819-*D17S1174* haplotype patterns. Representative results are shown in Figure 2D, and all the data are available on request. Various haplotype patterns were identified on the single, the duplicated, and the triplicated segments, and the [A-14] haplotype was most prevalent on the duplicated/triplicated segments (Table 1). While the distribution of CA repeat lengths on the single segments was discontinuous, similar discontinuous distribution was

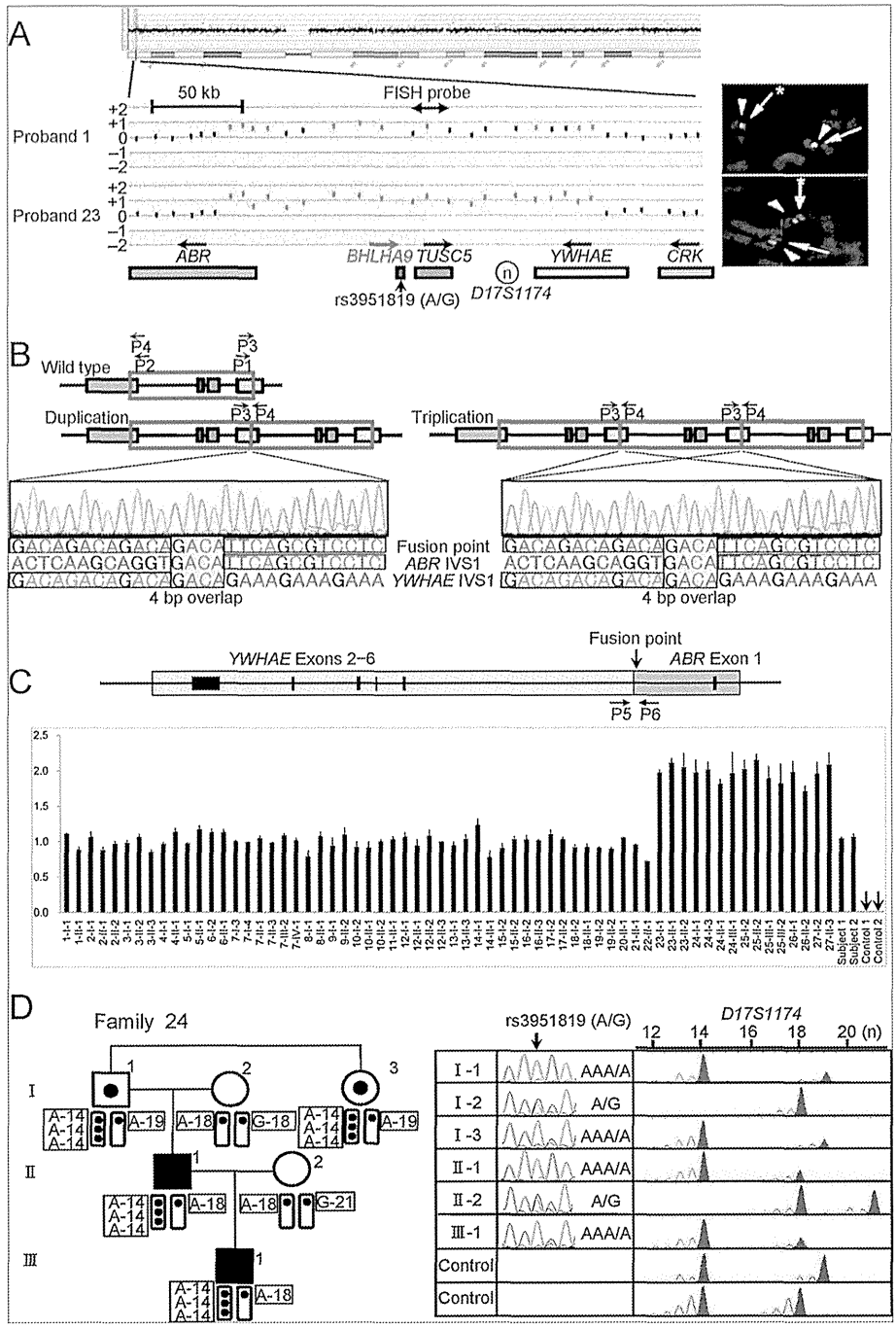

Figure 2 (See legend on next page.)

(See figure on previous page.)
Figure 2 Identification and characterization of the duplications/triplications involving *BHLHA9* at chromosome 17p13.3. A. Array CGH and FISH analyses in proband 1 and proband 23 with GWC. In array CGH analysis, the black and the red dots denote the normal and the increased copy numbers, respectively. Since the log2 signal ratios for a ~200 kb region encompassing *BHLHA9* are around +0.5 in the proband 1 and around +1.0 in the proband 23, this indicates the presence of three and four copies of this region in the two probands, respectively. In FISH analysis, two red signals with an apparently different density are detected by the 8,289 bp PCR probe (the stronger signals are indicated with asterisks). The green signals derive from an internal control probe (CEP17). The arrows on the genes show transcriptional directions. Rs3951819 (A/G) resides within *BHLHA9*. **B**. Determination of the fusion point. The fusion has occurred between intron 1 of *ABR* and intron 1 of *YWHAE*, and is associated with a 4 bp (GACA) microhomology. P1–P4 show the position of primers. **C**. Quantitative real-time PCR analysis. The upper part denotes the fusion point. P5 & P6 show the position of primers. The lower part shows the copy number of the fusion point in patients/subjects with duplications/triplications (indicated by a family-generation-individual style corresponding to that in Figure 1 and Additional file 5). Subject-1 and subject-2 denote the two control subjects with the duplication, and control-1 and control-2 represent normal subjects without the duplication/triplication. **D**. The rs3951819 (A/G SNP)–*D17S1174* (CA repeat number) haplotype patterns in family 24. Assuming no recombination between rs3951819 and *D17S1174*, the haplotype patterns of the family members are determined as shown here. The haplotype patterns of the remaining families have been interpreted similarly.

also observed in the Japanese general population (see Additional file 3).

Genomic environments around the breakpoints

The breakpoint on *YWHAE* intron 1 resided on a simple *Alu* repeat sequence, and that on *ABR* intron 1 was present on a non-repetitive sequence. There was no low copy repeat around the breakpoints. Comparison of the frequencies of known rearrangement-inducing DNA features between 600 bp sequences around the breakpoints and those of 48 regions selected at an interval of 1.5 Mb from chromosome 17 revealed that palindromes, several types of non-B DNA structures, and a rearrangement-associated sequence motif were abundant around the breakpoint on *YWHAE* intron 1 (see Additional file 4).

Clinical findings of families 1–27

Clinical assessment revealed several notable findings. First, duplications/triplications were associated with SHFM, SHFLD, GWC, or normal phenotype, with inter- and intra-familial clinical variability (Figure 1A). Second, in the 42 patients, split hand (SH) was more prevalent than split foot (SF) (41/42 vs. 17/42, $P = 6.2 \times 10^{-9}$), and long bone defect (LBD) was confined to lower extremities (0/42 vs. 13/42, $P = 4.1 \times 10^{-5}$) (Table 2 and Additional file 5). Third, there was no significant sex difference in the ratio between patients with limb malformations and patients/carriers with duplications/triplications (26/38 in males vs. 16/26 in females, $P = 0.60$) (Table 2 and Additional file 5). Fourth, the ratio of LBD positive families was significantly higher in triplications than in duplications (4/5 vs. 16/22, $P = 0.047$) (Figure 1A and Table 2). Fifth, while the duplications/triplications were transmitted from patients to patients, from carriers to patients, and from a carrier to a carrier (from I-1 to II-2 in family 12), transmission from a patient to a carrier was not identified (Figure 1A); it should be pointed out, however, that molecular analysis in a clinically normal child born to an affected parent was possible only in a single adult subject (II-1 in family 27), and that molecular analysis in clinically

Table 1 The rs3951819 (A/G SNP) – *D17S1174* (CA repeat number) haplotype

Patterns of the 210,050 bp segment subjected to copy number gains	
Haplotype pattern	**Family**
<Single segment>	
[A-14]	1, 5, 9, 15, 17, 19, 23, 26
[A-16]	12
[A-18]	3, 14, 15, 24, 25, 26
[A-19]	2, 6, 13, 19, 20, 24, 25, 27
[A-21]	5, 23
[G-12]	17
[G-14]	2, 3, 6, 12, 13, 19, 26
[G-18]	3, 5, 17, 18, 24, 25
[G-19]	9, 12, 18, 20, 25
[G-21]	1, 9, 19, 24, 27
[A-14] or [G-14]	16
[A-18] or [G-18]	4
[A-19] or [G-19]	4
[A-21] or [G-21]	16
<Duplicated segments>	
[A-14] + [A-14]	5, 12, 13, 14, 15, 20
[A-14] + [A-18]	1
[A-14] + [G-18] or [G-14] + [A-18]	2, 3, 4, 6, 9, 16, 17
[A-14] + [G-18] or [A-14] + [G-19]	18
[A-14] + [G-14] or [G-14] + [G-14]	19
<Triplicated segments>	
[A-14] + [A-14] + [A-14]	23, 24
[A-14] + [A-14] + [G-14]	25
[A-14] + [A-19] + [A-19]	26
[A-14] + [G-18] + [G-18] or [G-14] + [A-18] + [G-18]	27

The haplotype patterns written in the left column have been detected in at least one patient/subject in the families described in the right column.
Genotyping could not be performed in several patients/subjects who had been repeatedly examined previously, because of the extremely small amount of DNA samples that were virtually used up in the sequencing and array CGH analyses.

Table 2 Summary of clinical findings in patients/carriers with duplications/triplications involving *BHLHA9*

	SHFM (+) patients			LBD (+) patients			Patient ratio*			LBD (+) families		
	SH	SF	*P*-value	U-LBD	L-LBD	*P*-value	Male	Female	*P*-value	Trip	Dup	*P*-value
This study	41/42	17/42	6.2×10^{-9}	0/42	13/42	4.1×10^{-5}	26/38	16/26	0.60	4/5	16/22	0.047
Previous studies	63/84	23/84	8.6×10^{-10}	11/91	42/91	5.7×10^{-7}	68/114	31/79	5.7×10^{-3}	...	...	...
Sum	104/126	40/126	1.1×10^{-16}	11/133	55/133	3.0×10^{-10}	94/152	47/105	7.6×10^{-3}	...	...	...

SHFM: split-hand/foot malformation; SH: split hand; SF: split foot; LBD: long bone deficiency; U: upper; L: lower; Trip: triplication; and Dup: duplication.
In the previous studies, patients without detailed phenotypic description and those of unknown sex have been excluded (3–9).
*The ratio between patients with limb malformations and patients/carriers with duplications/triplications, i.e. the number of patients over the number of patients plus carriers.

normal children <20 years old was possible only in two subjects (II-2 in family 12 and II-1 in family 15). Lastly, limb malformation was inherited in an apparently autosomal dominant manner (from patients to patients), or took place as an apparently *de novo* event or as an apparently autosomal recessive trait (from clinically normal parents to a single or two affected children) (Figure 1A).

Attempts to identify a possible modifier(s)

The variable expressivity and incomplete penetrance in families 1–27 suggest the presence of a possible modifier (s) for the development of limb malformations. Thus, we performed further molecular studies in patients/subjects in whom DNA samples were still available, and compared the molecular data between patients with SHFM and those with SHFLD for the assessment of variable expressivity and between SHFM, SHFLD, or total patients and carriers for the evaluation of incomplete penetrance.

We first examined the possibility that the modifier(s) resides within or around *BHLHA9* (see Additional file 6). There was no *BHLHA9* mutation in all the 21 examined probands with SHFM, SHFLD, or GWC, as described in the section of "Sequence analysis of the known causative/candidate genes". The rs3951819 A/G SNP pattern on the duplicated/triplicated segments was apparently identical between patients and carriers (e.g. Figure 2D), and the frequency of A/G allele on the normal chromosome 17 was similar between SHFM and SHFLD patients and between SHFM, SHFLD, or total patients and carriers (see Additional file 7). The results of other known SNPs on *BHLHA9* (rs185242872, rs18936498, and rs140504068) were not informative, because of absence or extreme rarity of minor alleles. Furthermore, in SHFM families 7, 12, and 18, sequencing of a 7,406 bp region encompassing *BHLHA9* and Southern blot analysis using five probes and *Mfe*I-, *Ssp*I-, and *Sac*I-digested genomic DNA revealed no variation specific to the patients, and methylation analysis for a CpG rich region at the upstream of *BHLHA9* delineated massive hypomethylation in all the patients/carriers examined.

Next, we examined the possibility that a variant(s) of known causative genes constitutes the modifier(s). Since rs34201045 in *TP63* was identified in the mutation analysis, we compared rs34201045 genotyping data between the 27 probands and the 15 carriers. The allele and genotype frequencies were similar between SHFM and SHFLD patients and between SHFM, SHFLD, or total patients and carriers (see Additional file 8).

We finally performed exome sequencing in SHFM families 13 and 17–19. However, there was no variation specific to the patients. In addition, re-examination of the genomewide array CGH data showed no discernible copy number variation specific to the patients.

Discussion

BHLHA9 overdosage and clinical characteristics

We identified duplications/triplications of a ~ 200 kb genomic segment involving *BHLHA9* at 17p13.3 in 27 of 51 families with SHFM, SHFLD, or GWC. To our knowledge, this is the first study revealing the underlying genetic factor for the development of GWC, and demonstrating the presence of triplications involving *BHLHA9* that were suggested but not confirmed in the previous studies [5,9]. Furthermore, this study indicates that *BHLHA9*-containing duplications/triplications are the most frequent underlying factor for the development of limb malformations at least in Japan. Notably, SHFLD and GWC with LBD were significantly more frequent in patients with triplications than in those with duplications, and the duplications/triplications were identified in clinically normal familial members and in the general population. These findings imply that increased *BHLHA9* copy number constitutes a strong susceptibility, rather than a causative, factor with a dosage effect for the development of a range of limb malformations. Since *Bhlha9* is expressed in the developing ectoderm adjacent to the AER rather than the AER itself in mouse embryos [6], *BHLHA9* appears to play a critical role in the limb development by interacting with the AER. While the duplications/triplications identified in this study included *TUSC5* and generated an *ABR-YWHAE* chimeric gene (Figure 2C), *TUSC5* duplication and the chimeric gene formation are not common findings in the previously reported patients with duplications at 17p13.3 and SHFM and/or SHFLD [5-9]. In addition, none of *Tusc5*, *Abr*, and *Ywhae* is specifically expressed in the developing mouse limb buds [22] (A Transcriptome Atlas Database

for Mouse Embryo of Eurexpress Project, http://www.eurexpress.org/ee/project/).

Several clinical findings are noteworthy in patients/subjects with duplications/triplications. First, SH was more frequent than SF in this study as well as in the previous studies, and LBD was confined to lower extremities in this study and was more frequent in lower extremities than in upper extremities in the previous studies (Table 2) [4-10]. This implies that *BHLHA9* overdosage exerts differential effects on the different parts of limbs. Second, while limb malformations were similarly identified between males and females in this study, they were more frequently observed in males than in females in the previous studies (Table 2) [4-10]. In this regard, it has been reported that testosterone influences the digital growth pattern as indicated by the lower second to fourth digit length ratio in males than in females [23-25], and that Caucasian males have higher serum testosterone values and lower second to fourth digit length ratios than Oriental males [26,27]. Such testosterone effects on the digital growth pattern with ethnic difference may explain why male dominant manifestation was observed in the previous studies primarily from Caucasian countries and was not found in this study. Lastly, LBD was more prevalent in patients with triplications than in those with duplications. This suggests that LBD primarily occurs when the effects of *BHLHA9* overdosage are considerably elevated.

Genomic basis of the Japanese founder copy number gains

The duplications/triplications were associated with the same fusion point and variable haplotype patterns. Since there was no sequence homology or low-copy repeats around the breakpoints, it is unlikely that such duplications/triplications were recurrently produced in different individuals by non-allelic homologous recombination (NAHR) [17,20]. Instead, it is assumed that a Japanese founder duplication took place in a single ancestor, and was spread with subsequent triplication and modification of the haplotype patterns.

The most likely genomic basis of the Japanese duplications/triplications is illustrated in Additional file 9. Notably, a 4 bp (GACA) microhomology was identified at the duplication fusion point (Figure 2B). A microhomology refers to two to five nucleotides common to the sequences of the two breakpoints, and is found as an overlapping sequence at the join point [16,19,20]. This suggests that the Japanese founder duplication was generated by replication-based mechanisms such as fork stalling and template switching (FoSTeS) and microhomology-mediated break-induced replication (MMBIR), because the presence of such a microhomology is characteristic of FoSTeS/MMBIR [17-20]. Indeed, such a simple tandem duplication with a microhomology can be produced by one time FoSTeS/MMBIR [17-20], although it could also be generated by non-homologous end-joining (NHEJ) [17]. Since the [A-14] haplotype was most prevalent on the duplicated/triplicated segments, it is inferred that a genomic rearrangement occurred in an ancestor with the [A-14] haplotype, yielding the founder duplication with the [A-14] + [A-14] haplotype. Furthermore, the presence of multiple stimulants for genomic rearrangements around the breakpoint on *YWHAE* intron 1 would have facilitated the generation of the founder duplication. In particular, non-B structures are known to stimulate the occurrence of both replication-based FoSTeS/MMBIR and double-strand breaks and resultant NHEJ [17,28,29], although the relative importance of each non-B DNA structure is largely unknown.

Subsequent triplication and haplotype modification can develop from the Japanese founder duplication through unequal interchromatid and interchromosomal recombinations [17,20]. Indeed, a tandem triplication with the [A-14] + [A-14] + [A-14] haplotype can be generated by unequal exchange between sister chromatids with the [A-14] + [A-14] haplotype, and various haplotype patterns are yielded by unequal interchromosomal exchanges involving the duplicated or triplicated segments. Furthermore, the haplotype variation would be facilitated by unequal exchanges between sister chromatids harboring duplications/triplications with various haplotype patterns and by the further unequal interchromosomal exchanges.

Underlying factors for the phenotypic variability

The duplications/triplications were accompanied by limb malformations with variable expressivity and incomplete penetrance. Although this may suggest the presence of a possible modifier(s) for the development of limb malformations, such a modifier(s) was not detected. In particular, while patient-to-carrier transmission of duplications/triplications was not identified in this study, even patient-to-carrier-to-patient transmission has been reported in three pedigrees [5,6,10]. Such transmission pattern with incomplete penetrance characterized by skipping of a generation is apparently inexplicable by assuming a modifier (s) interacting with *BHLHA9* or independent of *BHLHA9* on the duplication/triplication positive chromosome 17, on the normal chromosome 17, or on other chromosomes (Figure 3, Models A, B, and C, see also the legends in Figure 3).

In this regard, it is noteworthy that the development of limb malformations is obviously dependent on the size of genomic segment subjected to copy number gains. Actually, limb malformation has occurred in only one of 21 large duplications encompassing *BHLHA9* (average 1.55 Mb, mean 1.12 Mb) and in 29 of 80 small duplications encompassing *BHLHA9* (average 244 kb, mean 263 kb) ($P = 5.9 \times 10^{-3}$) [8]. Consistent with this, the patients with large and

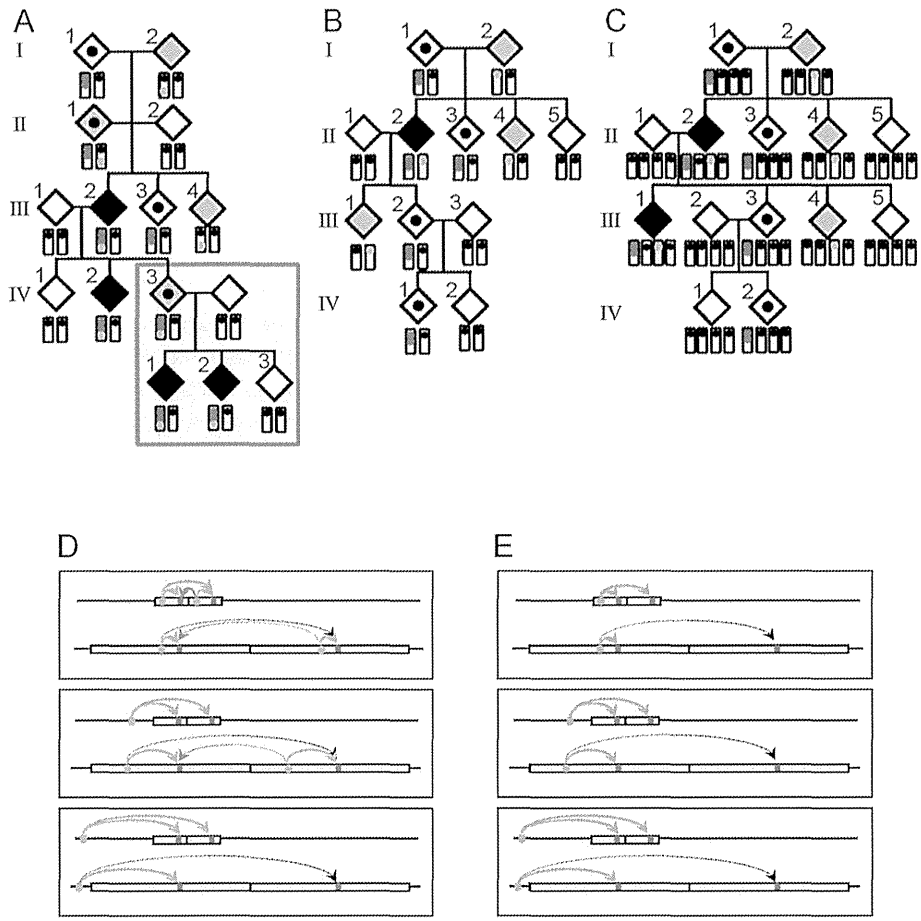

Figure 3 Models for a modifier(s) and effects of the duplication size. In models **A–C**, the yellow bars show chromosome 17, and the light green bars indicate other chromosomes. The two red dots represent the duplication at 17p13.3, and the blue dots indicate a putative modifier(s). Black painted diamonds represent limb malformation positive patients, dot-associated and gray painted diamonds indicate clinically normal carriers with the duplications and the modifier(s) respectively, and white painted diamonds denote clinically normal subjects without both the duplications and the modifier(s). **A**. This model assumes that co-existence of the duplication and a *cis*-acting modifier(s) causes limb malformation. If co-existence of the duplication and the *cis*-acting modifier(s) is associated with incomplete penetrance, this can explain all the transmission patterns observed to date, including the patient-to-carrier transmission and the presence of ≥ 2 affected children. **B**. This model postulates that the presence of a *cis*-acting modifier(s) on the normal chromosome 17 leads to limb malformation by enhancing the expression of the single *BHLHA9*, together with duplicated *BHLHA9* on the homologous chromosome. **C**. This model postulates that co-existence of the duplication at 17p13.3 and a modifier(s) on other chromosome causes limb malformation. In models **D–E**, the red bars represent *BHLHA9*, the blue circles indicate a physiological cis-regulatory element for *BHLHA9*, and the green circles indicate a non-physiological modifier(s) for *BHLHA9*. **D**. The physiological cis-regulatory element may be duplicated or non-duplicated, depending on its position relative to the size of the duplications. *BHLHA9* expression can be higher in small duplications than large duplications. **E**. The non-physiological modifier(s) can be transferred to various positions of the duplication positive chromosome 17, depending on the recombination places (see Model A). *BHLHA9* expression can be higher in small duplications than large duplications irrespective of the position of the modifier(s).

small duplications were ascertained primarily due to developmental retardation and limb malformation, respectively [8]. It is likely that a physiological cis-regulatory element for *BHLHA9* (e.g., an enhancer) can frequently but not invariably work on both of the duplicated *BHLHA9* when the duplication size is small but is usually incapable of working on duplicated *BHLHA9* when the duplication size is large, probably because of the difference in the chromatin structure (see Model D in Figure 3). Similar findings have also been reported in other genes. For example, small (~150 kb) and relatively small (600–800 kb) duplications involving a putative testis-specific enhancer(s) for *SOX9* have caused 46,XX testicular and ovotesticular disorders of sex development respectively, whereas large duplications (~2 Mb) involving the enhancer(s) have permitted normal ovarian development in 46,XX individuals [30].

Thus, a plausible explanation may be that a range of limb malformations emerge when the effects of *BHLHA9* overdosage exceed the threshold for the development of SHFM, SHFLD, or GWC, depending on the conditions of

other genetic and environmental factors including the size of duplications/triplications as an important but not definitive factor. One may argue that this notion is inconsistent with the apparent anticipation phenomenon that is suggested by the rare patient-to-carrier transmission and the frequent carrier-to-patient transmission of the duplications/triplications, because no specific factor(s) exaggerating the development of limb malformations is postulated in the next generation. However, the skewed transmission pattern would primarily be ascribed to ascertainment bias rather than anticipation [31]. Indeed, while clinically normal parents of disease positive children would frequently be examined for the underlying genetic factor(s) of the children, clinically normal children born to disease positive parents would not usually be studied for such factor(s), as exemplified in this study. Similarly, the frequent patient-to-patient transmission of the duplications/triplications would also be ascribed to ascertainment bias, because molecular studies would preferentially be performed in such families. Nevertheless, the apparently autosomal dominant inheritance pattern of limb malformations in several families may still suggest the relevance of a non-physiological *cis*-acting modifier(s) (see Models A and E in Figure 3). It is possible that such a modifier(s), once transferred onto the duplication/triplication positive chromosome 17, is usually co-transmitted with the duplications/triplications, leading to a specific condition in which the effects of *BHLHA9* overdosage frequently but not invariably exceed the threshold for the development of limb malformations in offsprings with the duplications/triplications.

Remarks

Several matters should be pointed out in the present study. First, in contrast to diverse duplication sizes in non-Japanese populations [5-9], the size of the genomic segment subjected to duplications/triplications was identical in this study. Since families 1–27 were derived from various places of Japan, there is no selection bias in terms of a geographic distribution. Rather, since the small duplications/triplications identified in this study were not associated with developmental retardation, it is likely that they spread throughout Japan primarily via carriers with normal fitness and were found via patients with limb malformations. Obviously, this notion does not exclude the possible presence of other types of duplications/triplications at 17p13.3 in Japan. Second, except for the duplications/triplications at 17p13.3, we could reveal a homozygous *WNT10B* mutation (SHFM6) only in a single SHFM family and chromosome 10q24 duplications (SHFM3) only in three SHFM families. Thus, underlying factors are still unknown in the remaining 20 families, although tiny deletions and/or duplications affecting the known SHFM loci might have been overlooked because of the low resolution of the array. In addition, although all the probands had a normal karyotype, there might be cryptic translocations and/or inversions involving the known SHFM loci. Third, no deletion of *BHLHA9* was identified in the 51 probands and in the 200 control subjects. This argues against the relevance of *BHLHA9* haploinsufficiency to limb malformations, and coincides with the Japanese founder duplication being produced by a replication-mediated mechanism rather than an interchromatid/interchromosomal (but not an intrachromatid) NAHR that can lead to both deletions and duplications as a mirror image [17]. Furthermore, it remains to be determined (i) whether gain-of-function mutations (and possibly loss-of-function mutations as well) of *BHLHA9* are identified in patients with limb malformations, (ii) whether duplications/triplications involving *BHLHA9* underlie limb malformations other than SHFM, SHFLD, and GWC, and (iii) whether *BHLHA9*-containing duplications/triplications are also the most frequent underlying factors for limb malformations in non-Japanese populations.

Conclusions

The results imply that (i) duplications/triplications involving *BHLHA9* at chromosome 17p13.3 constitute a strong susceptibility factor for the development of a range of limb malformations including SHFM, SHFLD, and GWC; (ii) the Japanese founder duplication was generated by a replication-based mechanism and spread with subsequent triplication and haplotype modification through recombination-based mechanisms; and (iii) clinical variability appears to be due to multiple factors including the size of duplications/triplications. Thus, the present study provides useful information on the development of limb malformations.

Additional files

Additional file 1: Table S1. Primers utilized in this study.

Additional file 2: Figure S1. Real-time PCR analysis.

Additional file 3: Figure S2. *D17S1174* analysis in 200 Japanese control subjects, showing discontinuous distribution of the CA repeat numbers, as observed in the Japanese families with limb malformations.

Additional file 4: Table S2. *In silico* analysis for specific structures around the breakpoint-flanking regions and control regions.

Additional file 5: Table S3. Phenotypes in patients/subjects with increased copy number of *BHLHA9*.

Additional file 6: Figure S3. Genomic region encompassing *BHLHA9* examined in this study.

Additional file 7: Table S4. Polymorphism analysis of rs3951819 (A/G SNP) in *BHLHA9*.

Additional file 8: Table S5. Polymorphism analysis of rs34201045 (4 bp insertion) in *TP63*.

Additional file 9: Figure S4. Genomic basis of the Japanese founder copy number gain.

Abbreviations

AER: Apical ectodermal ridge; CEP17: Centromere of chromosome 17; CGH: Comparative genomic hybridization; Dup: Duplication; FoSTeS: Fork stalling and template switching; GWC: Gollop-Wolfgang complex; L: Lower; LBD: Long bone defect; MMBIR: Microhomology-mediated break-induced replication; NAHR: Non-allelic homologous recombination; N.E.: Not examined; NHEJ: Non-homologous end-joining; qPCR: Quantitative real-time PCR; SF: Split foo17)t; SH: Split hand; SHFLD: SHFM with long bone deficiency; SHFM: Split-hand/foot malformation; Trip: Triplication; U: Upper.

Competing interests

The authors have nothing to declare.

Authors' contributions

Molecular analysis using human samples was performed by EN, HK, FK. RY, SN, SW, KY, TT, SS, MF, and TT, ST, and SY; clinical assessment and blood sampling by RK, HT, SM, TK, TH, MK, AS, KS, HO, NH, HN, EH, TN, HY, GN, and TO; design of this study and interpretations of the data by HA, SI, and TO; and paper writing by TO. All authors read and approved the final manuscript.

Acknowledgements

This work was supported in part by Grants-in-Aid for Scientific Research on Innovative Areas [22132004-A01] from the Ministry of Education, Culture, Sports, Science and Technology, by Grant for Research on Intractable Diseases from the Ministry of Health, Labor and Welfare [H24-048], and by Grants from National Center for Child Health and Development [23A-1, 24–7]. The funders had no role in study design, data collection and analysis, decision to publish, or preparation of the manuscript.

Author details

[1]Department of Pediatrics, Hamamatsu University School of Medicine, Hamamatsu 431-3192, Japan. [2]Laboratory of Bone and Joint Diseases, Center for Integrative Medical Sciences, RIKEN, Tokyo, Japan. [3]Department of Orthopedic Surgery, Tokyo, Japan. [4]Division of Medical Genetics, National Center for Child Health and Development, Tokyo, Japan. [5]Section of Clinical Genetics, Department of Pediatrics, Tenshi Hospital, Sapporo, Japan. [6]Department of Pediatrics, Central Hospital, Aichi Human Service Center, Kasugai, Japan. [7]Department of Human Genetics, Nagasaki University Graduate School of Biomedical Sciences, Nagasaki, Japan. [8]Department of Medical Genetics, Shinshu University School of Medicine, Matsumoto, Japan. [9]Department of Pediatrics, Keio University School of Medicine, Tokyo, Japan. [10]Department of Orthopedics, National Rehabilitation Center for Disabled Children, Tokyo, Japan. [11]Division of Medical Genetics, Saitama Children's Medical Center, Saitama, Japan. [12]Department of Rehabilitation Medicine, University of Tokyo, Tokyo, Japan. [13]Department of Genetic Counseling, Graduate School of Humanities and Sciences, Ochanomizu University, Tokyo, Japan. [14]Department of Orthopedic Surgery, Japanese Red Cross Nagoya Daiichi Hospital, Nagoya, Japan. [15]Department of Pediatrics, Dokkyo Medical University Koshigaya Hospital, Koshigaya, Japan. [16]Division of Medical Genetics, Tokyo, Japan. [17]Department of Pediatric Imaging, Tokyo Metropolitan Children's Medical Center, Tokyo, Japan. [18]Division of Neurology/Molecular Brain Science, Kobe University Graduate School of Medicine, Kobe, Japan. [19]Department of Systems Biomedicine, National Research Institute for Child Health and Development, Tokyo, Japan. [20]Department of Systems Biomedicine, Graduate School of Medical and Dental Sciences, Tokyo Medical and Dental University, Tokyo, Japan. [21]Department of Molecular Endocrinology, National Research Institute for Child Health and Development, Tokyo, Japan. [22]Present address: Laboratory of Metabolism Center for Cancer Research, National Cancer Institute, Bethesda, MD, USA.

Received: 15 April 2014 Accepted: 22 July 2014
Published online: 21 October 2014

References

1. Duijf PH, van Bokhoven H, Brunner HG: **Pathogenesis of split-hand/split-foot malformation.** *Hum Mol Genet* 2003, **12**:R51–60.
2. Gurrieri F, Everman DB: **Clinical, genetic, and molecular aspects of split-hand/foot malformation: an update.** *Am J Med Genet A* 2013, **161A**:2860–2672.
3. Lango Allen H, Caswell R, Xie W, Xu X, Wragg C, Turnpenny PD, Turner CL, Weedon MN, Ellard S: **Next generation sequencing of chromosomal rearrangements in patients with split-hand/split-foot malformation provides evidence for DYNC1/1 exonic enhancers of DLX5/6 expression in humans.** *J Med Genet* 2014, **51**:264–267.
4. Lezirovitz K, Maestrelli SR, Cotrim NH, Otto PA, Pearson PL, Mingroni-Netto RC: **A novel locus for split-hand/foot malformation associated with tibial hemimelia (SHFLD syndrome) maps to chromosome region 17p13.1-17p13.3.** *Hum Genet* 2008, **123**:625–631.
5. Armour CM, Bulman DE, Jarinova O, Rogers RC, Clarkson KB, DuPont BR, Dwivedi A, Bartel FO, McDonell L, Schwartz CE, Boycott KM, Everman DB, Graham GE: **17p13.3 microduplications are associated with split-hand/foot malformation and long-bone deficiency (SHFLD).** *Eur J Hum Genet* 2011, **19**:1144–1151.
6. Klopocki E, Lohan S, Doelken SC, Stricker S, Ockeloen CW, Soares Thiele de Aguiar R, Lezirovitz K, Mingroni Netto RC, Jamsheer A, Shah H, Kurth I, Habenicht R, Warman M, Devriendt K, Kordass U, Hempel M, Rajab A, Mäkitie O, Naveed M, Radhakrishna U, Antonarakis SE, Horn D, Mundlos S: **Duplications of BHLHA9 are associated with ectrodactyly and tibia hemimelia inherited in non-Mendelian fashion.** *J Med Genet* 2012, **49**:119–125.
7. Petit F, Andrieux J, Demeer B, Collet LM, Copin H, Boudry-Labis E, Escande F, Manouvrier-Hanu S, Mathieu-Dramard M: **Split-hand/foot malformation with long-bone deficiency and BHLHA9 duplication: two cases and expansion of the phenotype to radial agenesis.** *Eur J Med Genet* 2013, **56**:88–92.
8. Curry CJ, Rosenfeld JA, Grant E, Gripp KW, Anderson C, Aylsworth AS, Saad TB, Chizhikov VV, Dybose G, Fagerberg C, Falco M, Fels C, Fichera M, Graakjaer J, Greco D, Hair J, Hopkins E, Huggins M, Ladda R, Li C, Moeschler J, Nowaczyk MJ, Ozmore JR, Reitano S, Romano C, Roos L, Schnur RE, Sell S, Suwannarat P, Svaneby D, *et al*: **The duplication 17p13.3 phenotype: analysis of 21 families delineates developmental, behavioral and brain abnormalities, and rare variant phenotypes.** *Am J Med Genet A* 2013, **161A**:1833–1852.
9. Luk HM, Wong VC, Lo IF, Chan KY, Lau ET, Kan AS, Tang MH, Tang WF, She WM, Chu YW, Sin WK, Chung BH: **A prenatal case of split-hand malformation associated with 17p13.3 triplication - a dilemma in genetic counseling.** *Eur J Med Genet* 2014, **57**:81–84.
10. Petit F, Jourdain AS, Andrieux J, Baujat G, Baumann C, Beneteau C, David A, Faivre L, Gaillard D, Gilbert-Dussardier B, Jouk PS, Le Caignec C, Loget P, Pasquier L, Porchet N, Holder-Espinasse M, Manouvrier-Hanu S, Escande F: **Split hand/foot malformation with long-bone deficiency and BHLHA9 duplication: report of 13 new families.** *Clin Genet* 2014, **85**:464–469.
11. Kano H, Kurosawa K, Horii E, Ikegawa S, Yoshikawa H, Kurahashi H, Toda T: **Genomic rearrangement at 10q24 in non-syndromic split-hand/split-foot malformation.** *Hum Genet* 2005, **118**:477–483.
12. Matsuyama J, Mabuchi A, Zhang J, Iida A, Ikeda T, Kimizuka M, Ikegawa S: **A pair of sibs with tibial hemimelia born to phenotypically normal parents.** *J Hum Genet* 2003, **48**:173–176.
13. Kagami M, Sekita Y, Nishimura G, Irie M, Kato F, Okada M, Yamamori S, Kishimoto H, Nakayama M, Tanaka Y, Matsuoka K, Takahashi T, Noguchi M, Tanaka Y, Masumoto K, Utsunomiya T, Kouzan H, Komatsu Y, Ohashi H, Kurosawa K, Kosaki K, Ferguson-Smith AC, Ishino F, Ogata T: **Deletions and epimutations affecting the human 14q32.2 imprinted region in individuals with paternal and maternal upd(14)-like phenotypes.** *Nat Genet* 2008, **40**:237–242.
14. Iida A, Okamoto N, Miyake N, Nishimura G, Minami S, Sugimoto T, Nakashima M, Tsurusaki Y, Saitsu H, Shiina M, Ogata K, Watanabe S, Ohashi H, Matsumoto N, Ikegawa S: **Exome sequencing identifies a novel INPPL1 mutation in opsismodysplasia.** *J Hum Genet* 2013, **58**:391–394.
15. Cer RZ, Donohue DE, Mudunuri US, Temiz NA, Loss MA, Starner NJ, Halusa GN, Volfovsky N, Yi M, Luke BT, Bacolla A, Collins JR, Stephens RM: **Non-B DB v2.0: a database of predicted non-B DNA-forming motifs and its associated tools.** *Nucl Acids Res* 2013, **41**:D94–D100.
16. Kornreich R, Bishop DF, Desnick RJ: **α-Galactosidase A gene rearrangements causing Fabry disease: identification of short direct repeats at breakpoints in an Alu-rich gene.** *J Biol Chem* 1990, **265**:9319–9326.
17. Gu W, Zhang F, Lupski JR: **(2008) Mechanisms for human genomic rearrangements.** *Pathogenetics* 2008, **1**:4.
18. Vissers LE, Bhatt SS, Janssen IM, Xia Z, Lalani SR, Pfundt R, Derwinska K, de Vries BB, Gilissen C, Hoischen A, Nesteruk M, Wisniowiecka-Kowalnik B, Smyk

M, Brunner HG, Cheung SW, van Kessel AG, Veltman JA, Stankiewicz P: **Rare pathogenic microdeletions and tandem duplications are microhomology-mediated and stimulated by local genomic architecture.** *Hum Mol Genet* 2009, **18**:3579–3593.
19. Hastings PJ, Ira G, Lupski JR: **A microhomology-mediated break-induced replication model for the origin of human copy number variation.** *PLoS Genet* 2009, **5**:e1000327.
20. Colnaghi R, Carpenter G, Volker M, O'Driscoll M: **The consequences of structural genomic alterations in humans: genomic disorders, genomic instability and cancer.** *Semin Cell Dev Biol* 2011, **2011**(22):875–885.
21. Ugur SA, Tolun A: **Homozygous WNT10b mutation and complex inheritance in Split-Hand/Foot Malformation.** *Hum Mol Genet* 2008, **17**:2644–2653.
22. Oort PJ, Warden CH, Baumann TK, Knotts TA, Adams SH: **Characterization of Tusc5, an adipocyte gene co-expressed in peripheral neurons.** *Mol Cell Endocrinol* 2007, **276**:24–35.
23. Manning JT, Scutt D, Wilson J, Lewis-Jones DI: **The ratio of 2nd to 4th digit length: a predictor of sperm numbers and concentrations of testosterone, luteinizing hormone and oestrogen.** *Hum Reprod* 1998, **13**:3000–3004.
24. Manning JT, Trivers RL, Singh D, Thornhill R: **The mystery of female beauty.** *Nature* 1999, **399**:214–215.
25. Williams TJ, Pepitone ME, Christensen SE, Cooke BM, Huberman AD, Breedlove NJ, Breedlove TJ, Jordan CL, Breedlove SM: **Finger-length ratios and sexual orientation.** *Nature* 2000, **404**:455–456.
26. Heald AH, Ivison F, Anderson SG, Cruickshank K, Laing I, Gibson JM: **Significant ethnic variation in total and free testosterone concentration.** *Clin Endocrinol* 2003, **58**:262–266.
27. Manning JT, Stewart A, Bundred PE, Trivers RL: **Sex and ethnic differences in 2nd to 4th digit ratio of children.** *Early Hum Dev* 2004, **80**:161–168.
28. Wang G, Vasquez KM: **Non-B DNA structure-induced genetic instability.** *Mutat Res* 2006, **598**:103–119.
29. Zhao J, Bacolla A, Wang G, Vasquez KM: **Non-B DNA structure-induced genetic instability and evolution.** *Cell Mol Life Sci* 2010, **67**:43–62.
30. Benko S, Gordon CT, Mallet D, Sreenivasan R, Thauvin-Robinet C, Brendehaug A, Thomas S, Bruland O, David M, Nicolino M, Labalme A, Sanlaville D, Callier P, Malan V, Huet F, Molven A, Dijoud F, Munnich A, Faivre L, Amiel J, Harley V, Houge G, Morel Y, Lyonnet S: **Disruption of a long distance regulatory region upstream of SOX9 in isolated disorders of sex development.** *J Med Genet* 2011, **48**:825–830.
31. Fraser FC: **Trinucleotide repeats not the only cause of anticipation.** *Lancet* 1997, **350**:459–460.

doi:10.1186/s13023-014-0125-5
Cite this article as: Nagata *et al.*: Japanese founder duplications/triplications involving *BHLHA9* are associated with split-hand/foot malformation with or without long bone deficiency and Gollop-Wolfgang complex. *Orphanet Journal of Rare Diseases* 2014 **9**:125.

ORIGINAL RESEARCH ARTICLE | Genetics inMedicine

Open

Comprehensive and quantitative multilocus methylation analysis reveals the susceptibility of specific imprinted differentially methylated regions to aberrant methylation in Beckwith–Wiedemann syndrome with epimutations

Toshiyuki Maeda, MD[1,2], Ken Higashimoto, PhD[1], Kosuke Jozaki, PhD[1], Hitomi Yatsuki, PhD[1], Kazuhiko Nakabayashi, PhD[3], Yoshio Makita, PhD[4], Hidefumi Tonoki, PhD[5], Nobuhiko Okamoto, MD[6], Fumio Takada, PhD[7], Hirofumi Ohashi, PhD[8], Makoto Migita, PhD[9], Rika Kosaki, MD[10], Keiko Matsubara, PhD[11], Tsutomu Ogata, PhD[12], Muneaki Matsuo, PhD[2], Yuhei Hamasaki, PhD[2], Yasufumi Ohtsuka, MD[1,2], Kenichi Nishioka, PhD[1], Keiichiro Joh, PhD[1], Tsunehiro Mukai, PhD[13], Kenichiro Hata, PhD[3] and Hidenobu Soejima, PhD[1]

Purpose: Expression of imprinted genes is regulated by DNA methylation of differentially methylated regions (DMRs). Beckwith–Wiedemann syndrome is an imprinting disorder caused by epimutations of DMRs at 11p15.5. To date, multiple methylation defects have been reported in Beckwith–Wiedemann syndrome patients with epimutations; however, limited numbers of DMRs have been analyzed. The susceptibility of DMRs to aberrant methylation, alteration of gene expression due to aberrant methylation, and causative factors for multiple methylation defects remain undetermined.

Methods: Comprehensive methylation analysis with two quantitative methods, matrix-assisted laser desorption/ionization mass spectrometry and bisulfite pyrosequencing, was conducted across 29 DMRs in 54 Beckwith–Wiedemann syndrome patients with epimutations. Allelic expressions of three genes with aberrant methylation were analyzed. All DMRs with aberrant methylation were sequenced.

Results: Thirty-four percent of *Kv*DMR1–loss of methylation patients and 30% of *H19*DMR–gain of methylation patients showed multiple methylation defects. Maternally methylated DMRs were susceptible to aberrant hypomethylation in *Kv*DMR1–loss of methylation patients. Biallelic expression of the genes was associated with aberrant methylation. *Cis*-acting pathological variations were not found in any aberrantly methylated DMR.

Conclusion: Maternally methylated DMRs may be vulnerable to DNA demethylation during the preimplantation stage, when hypomethylation of *Kv*DMR1 occurs, and aberrant methylation of DMRs affects imprinted gene expression. *Cis*-acting variations of the DMRs are not involved in the multiple methylation defects.

Genet Med advance online publication 8 May 2014

Key Words: Beckwith–Wiedemann syndrome; DNA methylation; differentially methylated region; genomic imprinting; multiple methylation defects

INTRODUCTION

Genomic imprinting is an epigenetic phenomenon that leads to parent-specific differential expression of a subset of mammalian genes. Most imprinted genes are clustered in regions called imprinting domains, and the expression of imprinted genes within these domains is regulated by imprinting control regions.[1,2] Differentially methylated regions (DMRs), which are defined as having DNA methylation on only one of the two parental alleles, play critical roles in the regulation of imprinting. There are two kinds of DMRs: maternally methylated DMRs (matDMRs) and paternally methylated DMRs (patDMRs). In addition, there is another classification, gametic DMRs and somatic DMRs, based on the timing of the establishment of differential methylation. Gametic DMRs acquire DNA methylation during gametogenesis, and the methylation is maintained from zygote to somatic cells during all developmental stages. Most gametic DMRs are identical to imprinting control regions. On the other hand, somatic DMRs are established during early embryogenesis after fertilization under the control of nearby imprinting control regions.[1,2] Because imprinted genes play an important role in the growth and development of embryos, placental formation, and metabolism, aberrant expression of

[1]Division of Molecular Genetics and Epigenetics, Department of Biomolecular Sciences, Faculty of Medicine, Saga University, Saga, Japan; [2]Department of Pediatrics, Faculty of Medicine, Saga University, Saga, Japan; [3]Department of Maternal–Fetal Biology, National Research Institute for Child Health and Development, Tokyo, Japan; [4]Education Center, Asahikawa Medical University, Asahikawa, Japan; [5]Department of Pediatrics, Maternal, Perinatal, and Child Medical Center, Tenshi Hospital, Sapporo, Japan; [6]Department of Medical Genetics, Osaka Medical Center and Research Institute for Maternal and Child Health, Izumi, Japan; [7]Department of Medical Genetics, Kitasato University Graduate School of Medical Sciences, Kanagawa, Japan; [8]Division of Medical Genetics, Saitama Children's Medical Center, Saitama, Japan; [9]Department of Pediatrics, Nippon Medical School, Tokyo, Japan; [10]Division of Medical Genetics, National Center for Child Health and Development, Tokyo, Japan; [11]Department of Molecular Endocrinology, National Research Institute for Child Health and Development, Tokyo, Japan; [12]Department of Pediatrics, Hamamatsu University School of Medicine, Hamamatsu, Japan; [13]Nishikyushu University, Saga, Japan. Correspondence: Hidenobu Soejima (soejimah@cc.saga-u.ac.jp)

Submitted 10 November 2013; accepted 7 April 2014; advance online publication 8 May 2014. doi:10.1038/gim.2014.46

imprinted genes due to epigenetic or genetic abnormalities is implicated in the pathogenesis of some human disorders, such as congenital anomalies and tumors.[1,2]

Beckwith–Wiedemann syndrome (BWS; Online Mendelian Inheritance in Man (OMIM) #130650) is an imprinting disease that is characterized by prenatal and postnatal macrosomia, macroglossia, abdominal wall defects, and variable minor features. The relevant imprinted chromosomal region in BWS is 11p15.5, which consists of two imprinted domains, *IGF2/H19* and *CDKN1C/KCNQ1OT1*, *H19*DMR and *Kv*DMR1 being the respective imprinting control regions.[3–5] Among several causative alterations identified so far, loss of methylation (LOM) at *Kv*DMR1 and gain of methylation (GOM) at *H19*DMR are isolated epimutations. Hypomethylation at multiple imprinted DMRs has been reported in patients with transient neonatal diabetes mellitus type 1,[6] and the same phenomenon, referred to as multiple methylation defects (MMDs), has been reported in BWS patients with *Kv*DMR1-LOM.[7–13] However, although the human genome contains more than 30 imprinting domains (http://www.geneimprint.com), a limited number of imprinted DMRs have been analyzed so far, with the exception of a report by Court et al.[12] In addition, methods used for methylation analysis have ranged from nonquantitative to quantitative approaches, and although some studies have used only one method for methylation analysis,[8,9,11] others have used two or more in conjuction.[7,10–13] Furthermore, the questions of whether susceptibility to aberrant methylation is different in each type of DMR, whether aberrant methylation indeed affects imprinted gene expression, and what causative factors are responsible for MMDs still remain unanswered. To clarify these issues, we have conducted a comprehensive methylation screening in BWS patients with *Kv*DMR1-LOM or *H19*DMR-GOM with a quantitative method, matrix-assisted laser desorption/ionization mass spectrometry (MALDI-TOF MS), on 29 imprinted DMRs, which represents the largest number of DMRs analyzed to date, followed by confirmation with another quantitative method, bisulfite pyrosequencing. We also performed gene expression analysis and sequencing of aberrantly methylated DMRs. We found that matDMRs are susceptible to aberrant methylation. We also found alterations in imprinted gene expression due to the aberrant methylation and no *cis*-acting pathological variations in DMRs with MMDs.

MATERIALS AND METHODS

Patients

Fifty-four BWS patients (25 boys, 26 girls, 3 gender-unspecified patients; average age: 3.0 years (0–13.9 years)) and their parents were enrolled in this study. Among them, 46 patients met clinical criteria for BWS as described by Weksberg et al.[3] and 6 patients met clinical criteria as described by DeBaun et al.[14] (**Supplementary Table S1** online). Because two patients were clinically diagnosed more than 20 years ago, their specific diagnostic criteria were unknown. The methylation statuses of *H19*DMR and *Kv*DMR1, paternal uniparental disomy of chromosome 11 (upd(11)pat), and *CDKN1C* mutations were screened as described previously.[15–17] Peripheral blood samples of most patients were subjected to standard G-banding chromosome analysis and/or high-resolution G-band patterning of human chromosome 11, but neither assay showed any abnormalities in any patient (data not shown). Among the 54 patients, 44 displayed *Kv*DMR1-LOM but did not show other causative alterations, including *H19*DMR-GOM, upd(11)pat, and *CDKN1C* mutations (data not shown). The remaining 10 patients displayed *H19*DMR-GOM but did not show other causative alterations (data not shown). We sequenced the entire *H19*DMR in *H19*DMR-GOM patients and found no mutations.[18] We used the peripheral blood samples of 24 children (11 boys, 13 girls; average age: 3.8 years (range of 0–8 years)) who visited the Department of Pediatrics, Saga University Hospital, as normal controls having only mild illness such as common cold. This study was approved by the Ethics Committee for Human Genome and Gene Analyses of the Faculty of Medicine, Saga University. Written informed consent was obtained from the parents or the guardians of the patients and participants.

DNA isolation and bisulfite conversion

Genomic DNA was extracted from the peripheral blood of patients using the FlexiGene DNA Kit (Qiagen, Hilden, Germany) according to the manufacturer's instructions. A total of 1 μg of genomic DNA was subjected to bisulfite conversion using the EZ DNA Methylation Kit (Zymo Research, Irvine, CA), and then the converted DNA was eluted in 100 μl of water. Unmethylated control DNA was created by whole-genome amplification using the REPLI-g Mini Kit (Qiagen). To prepare fully methylated control DNA, the unmethylated DNA created by whole-genome amplification was treated twice with *Sss*I methylase.

Methylation analysis by MALDI-TOF MS

The DNA methylation status of imprinted DMRs was analyzed by MALDI-TOF MS analysis with a MassARRAY system (Sequenom, San Diego, CA) as previously described.[19,20] Briefly, each DMR was amplified by bisulfite-mediated polymerase chain reaction (PCR) using a primer set containing a primer carrying the T7 promoter sequence at the 5′ end. In vitro transcription of the PCR product was performed with T7 RNA polymerase, and the transcript was subjected to uracil-specific cleavage with RNase A. MALDI-TOF MS analysis of the cleaved fragments produced signal pattern pairs indicative of nonmethylated and methylated DNA. Epityper software (Sequenom) analysis of the signals yielded a methylation index (MI) ranging from 0 (no methylation) to 1 (full methylation) for each CpG unit, which contained one or more CpG sites. Aberrant methylation of a CpG unit was defined as the condition in which the difference of MIs between each patient and the average of normal controls exceeded 0.15. This definition was based on our finding in methylation-sensitive Southern blots, which revealed that the differences in MI for *Kv*DMR1-LOM or *H19*DMR-GOM in BWS patients were ≥0.15 (data not shown). Because the analyzed DMRs included several CpG units, aberrant methylation of each DMR was defined as the situation in which more

than 60% of the total number of analyzed CpG units showed aberrant methylation (with the MI difference exceeding 0.15). In the case of *IGF2*-DMR0, the three CpG sites were analyzed based on previous reports.[21,22] All primers used in this study are shown in **Supplementary Table S2** online.

Methylation analysis by bisulfite pyrosequencing

The aberrant methylation status of DMRs identified by MALDI-TOF MS was confirmed by bisulfite pyrosequencing using QIAGEN PyroMark Q24 according to the manufacturer's instructions (Qiagen). Primers for bisulfite-mediated PCR and pyrosequencing were designed using PyroMark Assay Design 2.0 (Qiagen). In analogy with MALDI-TOF MS analysis, aberrant methylation of a CpG site was defined as the situation in which the difference of MIs between each patient and the average of normal controls exceeded 0.15. Aberrant methylation of each DMR was defined as the condition in which more than 60% of the total number of analyzed CpG sites showed aberrant methylation (with the MI difference exceeding 0.15).

Bisulfite sequencing

Bisulfite sequencing was performed to analyze allelic methylation of *ZDBF2*-DMR. After PCR amplification, the PCR products were cloned into a pT7Blue T-Vector (Novagen, Darmstadt, Germany), and individual clones were sequenced. Parental alleles were distinguished by a single-nucleotide polymorphism (SNP, *rs1861437*) within the DMR.

Expression analysis of *ZDBF2*, *FAM50B*, and *GNAS1A*

Total RNA was extracted from the peripheral blood of patients using the QIAamp RNA Blood Mini Kit (Qiagen). The RNA was treated with RNase-free DNase I, and reverse transcription was performed with random primers. We used SNPs for allelic expression to distinguish between the two parental alleles: *rs10932150* in exon 5 of *ZDBF2*; *rs6597007* in exon 2 of *FAM50B*; and *rs143800311*, which is a 5-bp deletion/insertion variation in exon 1A of *GNAS1A*. Reverse transcription–PCR (RT-PCR) products encompassing the SNPs of *ZDBF2* and *FAM50B* were directly sequenced. The products encompassing the deletion/insertion variation of *GNAS1A* were separated by electrophoresis on an Applied Biosystems 3130 genetic analyzer (Applied Biosystems, Foster City, CA) and then analyzed with GeneMapper software (Applied Biosystems). Total expression levels of *ZDBF2* and *FAM50B* were quantitated by real-time PCR with TaqMan probes (Applied Biosystems). The expression level of each gene was normalized against that of the housekeeping genes encoding hydroxymethylbilane synthase (*HMBS*) and glyceraldehyde-3-phosphate dehydrogenase (*GAPDH*). All quantitative RT-PCRs were performed in triplicate.

Sequencing of aberrantly methylated DMRs

Direct sequencing of all DMRs showing aberrant methylation in *Kv*DMR1-LOM patients was performed to determine whether there was any pathological variation.

Statistical analyses

Fisher's exact test was used for the comparison of aberrant methylated DMRs. Fisher's exact test or Mann–Whitney *U*-test was used for statistical analyses of clinical features between MMDs and monolocus methylation defects in *Kv*DMR1-LOM patients. A P value < 0.05 was considered statistically significant.

RESULTS

Validation of methylation analyses, MALDI-TOF MS, and bisulfite pyrosequencing

First, we selected 37 regions reported previously as imprinted DMRs in the human genome[16,20,23] (refer to http://www.geneimprint.com/). To validate the quantitative capability of MALDI-TOF MS methylation analysis, mixtures of the unmethylated control DNA and the fully methylated control DNA (0, 25, 50, 75, and 100% methylated DNA) were subjected to bisulfite conversion and analyzed. We found a significant correlation between the measured MIs and predicted MIs in all DMRs, except for *GRB10*, *PEG13*, and IG-DMR-CG4 (**Supplementary Figure S1** online). Furthermore, in normal leukocytes, two regions (*TCEB3C*, *USP29*) showed mostly full methylation and three regions (*TP73*, *SPTBN1*, *WT1-AS*) showed mostly no methylation, suggesting that these regions were not differentially methylated in leukocytes (data not shown). Therefore, we excluded these eight regions and decided to analyze the remaining 29 DMRs by MALDI-TOF MS. Second, we obtained MIs from 24 normal controls using MALDI-TOF MS and calculated the average and SD of each CpG unit. We excluded CpG units in which SDs were >0.1 from further analysis. Averages and SDs of all CpG units analyzed in this study are shown in **Supplementary Table S3** online. After the MALDI-TOF MS analysis, we used bisulfite pyrosequencing to confirm the aberrant methylation uncovered. We also obtained MIs from the 24 controls using bisulfite pyrosequencing and calculated the average and SD of each CpG site. We excluded one CpG site in *H19*DMR because its SD was >0.1 due to a known SNP (*rs10732516*). Averages and SDs of control CpG sites are shown in **Supplementary Table S3** online. Finally, we compared the MIs of MALDI-TOF MS and bisulfite pyrosequencing of each DMR and found a significant correlation (**Supplementary Figure S2** online).

Multilocus methylation defects in BWS patients with epimutations

Among the 44 *Kv*DMR1-LOM patients, 15 (34.1%) showed aberrantly methylated DMRs outside of *Kv*DMR1: six showed aberrant methylation at only one DMR, and the other nine showed two or more methylated DMRs (Figure 1a and **Supplementary Figure S3** online). The greatest number of aberrantly methylated DMRs was found in patient BWS-s113, who exhibited 12 DMRs. Most of the aberrantly methylated DMRs demonstrated LOM, which was seen at *ARHI*-CG1, *ARHI*-CG2, *ARHI*-CG3, *FAM50B*, *ZAC*, *IGF2R*-DMR2, *MEST*, *NNAT*, *L3MBTL1*, *NESPAS*, *GNASXL*, and *GNAS1A*. Among them, the most frequently hypomethylated DMRs were

ARHI-CG1 and *ARHI*-CG3, found in nine (20.5%) and eight (18.2%) patients, respectively. By contrast, three DMRs, located at *ZDBF2*, *NESP*, and *MCTS2*, showed GOM, which was found in six (13.6%), two (4.5%), and one (2.3%) patients, respectively. *GNASXL*-DMR showed GOM in one patient (2.3%), whereas four patients (9.1%) showed LOM. The other 13 DMRs were not aberrantly methylated in any *Kv*DMR1-LOM patient.

Among the 10 *H19*DMR-GOM patients, all patients showed GOM at the *H19* promoter DMR, which was usually observed with loss of imprinting of *IGF2* (Figure 1b).[24] Four patients showed GOM at either *IGF2*-DMR0 or *IGF2*-DMR2; two patients showed GOM at both. Moreover, both LOM and GOM at other DMRs were found: LOM was found at *INPP5Fv2*-DMR in patients BWS-s015 and BWS-s064, and GOM was found at *NESP*-DMR in patient BWS-s012.

In addition, to exclude aberrantly methylated DMRs resulting from chromosome abnormalities such as uniparental disomy and copy number abnormality, microsatellite analyses using patients' and their parents' DNA were performed on all DMRs showing aberrant methylation. For quantitative analyses, tetranucleotide repeat markers near the imprinted DMRs were used (**Supplementary Materials and Methods** online). We found that no DMRs, except for six DMRs in three patients, exhibited any chromosome abnormalities (summarized in **Supplementary Figure S4** online). These results strongly suggest that the aberrant methylation of DMRs observed was

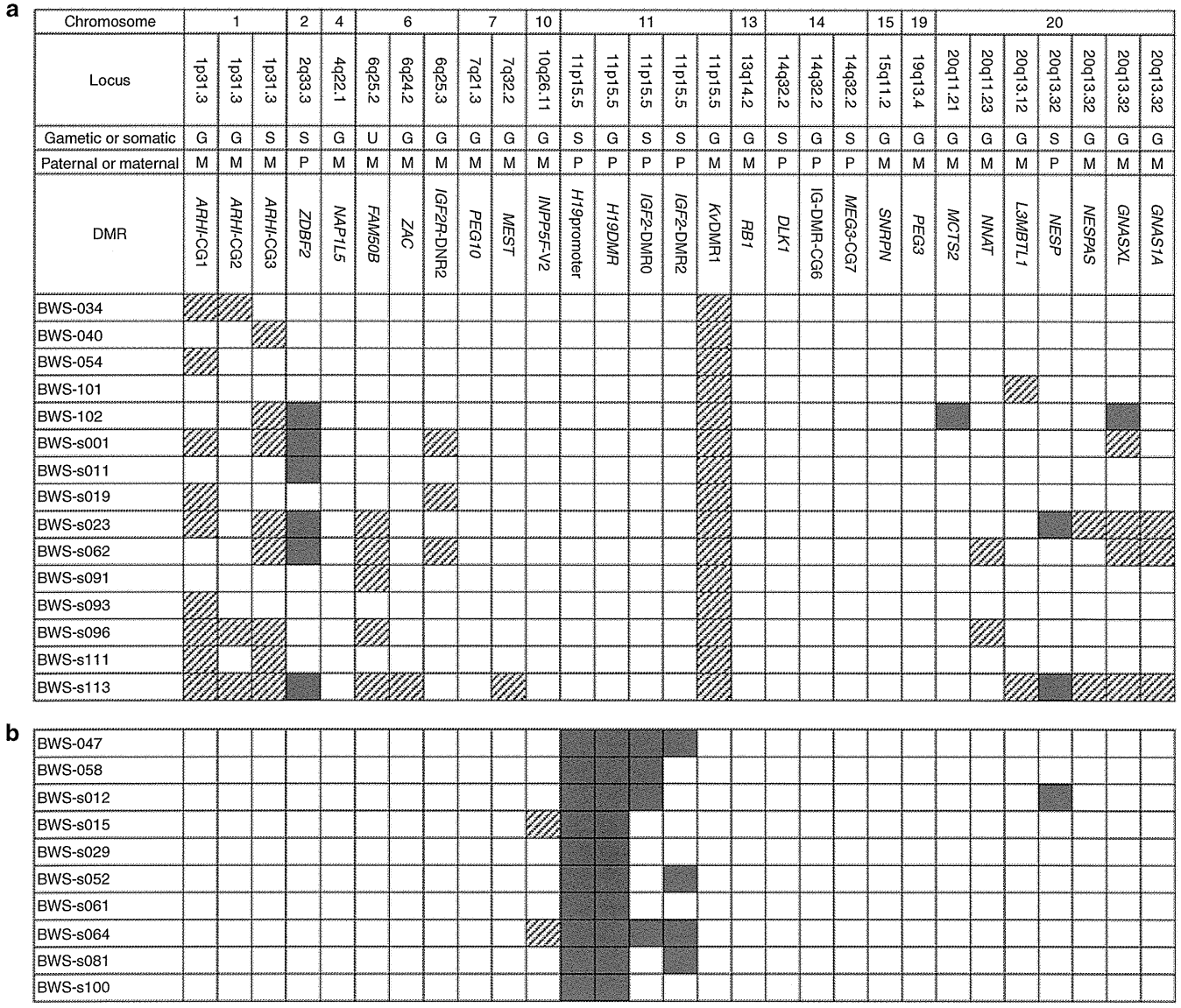

Figure 1 Results of methylation analyses of 29 imprinted differentially methylated regions (DMRs) in Beckwith–Wiedemann syndrome patients with epimutations. (**a**) Results of patients with *Kv*DMR1-LOM. Only the results of multiple methylation defects are shown. Aberrant methylation was confirmed by two quantitative methods: matrix-assisted laser desorption/ionization mass spectrometry and bisulfite pyrosequencing. The definition of aberrant methylation used here is described in the Materials and Methods section. Shaded rectangle: aberrant hypomethylation; dark gray rectangle: aberrant hypermethylation. (**b**) Results of all patients with *H19*DMR-GOM. GOM, gain of methylation; LOM, loss of methylation.

an isolated epimutation and was not due to chromosome abnormalities.

Comparison of aberrantly methylated DMRs

We found that 34.1% (15 of 44) of *Kv*DMR1-LOM patients and 30.0% (3 of 10) of *H19*DMR-GOM patients showed MMDs (**Figure 1a**). There was no statistical difference between them ($P > 0.99$, Fisher's exact test).

Among the 29 DMRs analyzed, there were 20 gametic DMRs and 8 somatic DMRs (**Figure 1a**). The timing of methylation establishment of one DMR (*FAM50B*-DMR) has not yet been determined. On the other hand, there were 20 matDMRs and 9 patDMRs. We investigated whether susceptibility to aberrant methylation differed for each type of DMR in *Kv*DMR1-LOM patients. *Kv*DMR1 itself, a gametic and matDMR, was excluded from this analysis. Several DMRs were mapped to certain imprinted domains, e.g., three DMRs in the *ARHI* domain and four in the *GNAS* domain. However, these DMRs differed by type, and aberrant methylations of these DMRs were not always linked. We also had previously found that DMRs in the *GNAS* domain were independently aberrantly methylated in hepatoblastoma.[20] Therefore, we decided to perform statistical analyses assuming the independence of each DMR.

We first compared gametic DMRs with somatic DMRs and found no significant difference in susceptibility ($P = 0.42$, Fisher's exact test; **Figure 2a**). *FAM50B*-DMR was excluded from this comparison. By contrast, matDMRs were aberrantly methylated more frequently than patDMRs ($P = 0.042$, Fisher's exact test; **Figure 2b**). In addition, among the aberrantly methylated DMRs, 12 showed LOM and 4 showed GOM. When we compared LOM with GOM, LOM preferentially occurred on matDMRs ($P = 0.050$, Fisher's exact test; **Figure 2c**). In this subanalysis, *GNASXL*-DMR was counted as having both GOM and LOM (**Figure 1a**). Furthermore, among the 12 DMRs with LOM, most of them (10) were gametic DMRs. These results suggest that matDMRs are susceptible to aberrant methylation and that gametic maternally methylated DMRs tend to be susceptible to LOM in *Kv*DMR1-LOM patients.

Biallelic expression of imprinted genes induced by aberrant methylation at their corresponding DMRs

We continued our investigation by determining whether allelic expression was associated with the methylation status of the corresponding DMR. We selected three genes (*ZDBF2*, *FAM50B*, and *GNAS1A*) expressed in lymphocytes.[25–27] In the case of *ZDBF2*, bisulfite sequencing of *ZDBF2*-DMR showed paternal monoallelic methylation in normal controls heterozygous for a specific SNP (*rs1861437*), whereas four BWS patients with GOM showed biallelic methylation: these findings were consistent with the results of MALDI-TOF MS and bisulfite pyrosequencing (**Figure 3a,b** and **Supplementary Figure S5** online). Because paternal expression of the *ZDBF2* gene is coupled with methylation of *ZDBF2*-DMR on the paternal allele,[25] biallelic expression due to biallelic methylation was expected. Indeed, three BWS patients heterozygous for a coding SNP (*rs10932150*) with hypermethylated DMRs clearly showed biallelic expression, in contrast with the paternal monoallelic expression in patients with normally methylated DMRs (**Figure 3c**). *FAM50B* and *GNAS1A* were paternally expressed and were coupled with maternal methylation of corresponding DMRs. RT-PCR using coding SNPs (*rs6597007* for *FAM50B* and *rs143800311* for *GNAS1A*) revealed that both genes were expressed biallelically with LOM of each corresponding DMR, which was in contrast with monoallelic expression in the patients with normally methylated DMRs (**Figure 4** and **Supplementary Figure S5** online). It is intriguing that *FAM50B* in patient BWS-s096 and *GNAS1A* in patient BWS-s062 were expressed from the maternal allele despite low-grade LOM,

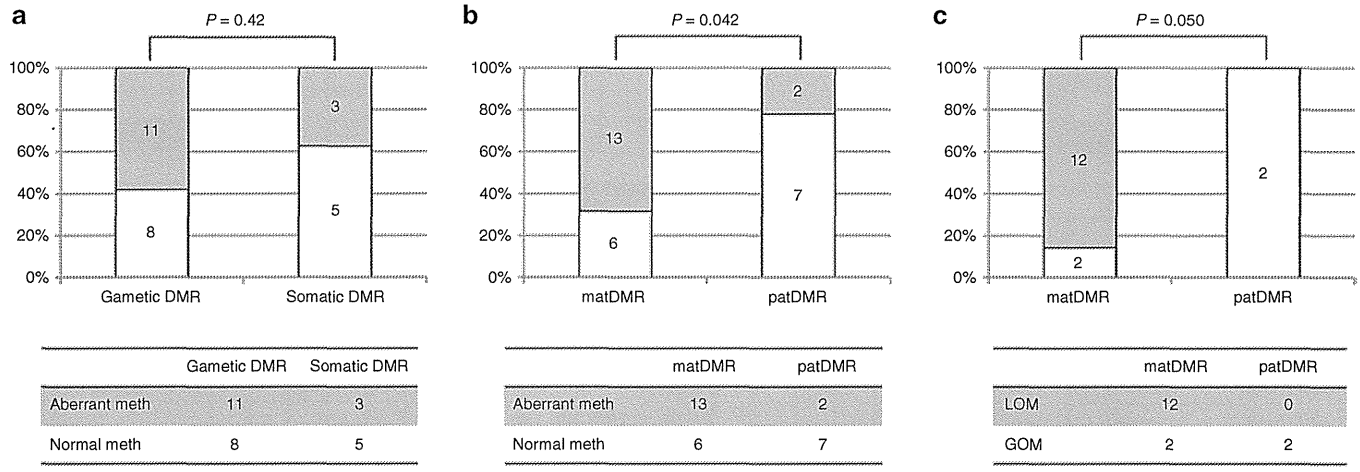

	Gametic DMR	Somatic DMR
Aberrant meth	11	3
Normal meth	8	5

	matDMR	patDMR
Aberrant meth	13	2
Normal meth	6	7

	matDMR	patDMR
LOM	12	0
GOM	2	2

Figure 2 Statistical analyses of aberrantly methylated differentially methylated region (DMRs). (**a**) Comparison of the number of aberrantly methylated DMRs between gametic DMRs and somatic DMRs in *Kv*DMR1-LOM patients. There was no statistical difference between the two DMRs ($P = 0.42$, Fisher's exact test). (**b**) Comparison of the number of aberrantly methylated DMRs between matDMRs and patDMRs in *Kv*DMR1-LOM patients. matDMRs were aberrantly methylated more frequently than patDMRs ($P = 0.042$, Fisher's exact test). (**c**) Comparison of the number of LOMs and GOMs between matDMRs and patDMRs among the aberrantly methylated DMRs in *Kv*DMR1-LOM patients. LOM preferentially occurred on matDMRs ($P = 0.050$, Fisher's exact test). GOM, gain of methylation; LOM, loss of methylation; matDMR, maternally methylated DMR; patDMR, paternally methylated DMR.